

## REPORT DOCUMENTATION PAGE

1a. REPORT SECURITY CLASSIFICATION  
Unclassified

ACTIVE MARKINGS

None

2a. SECURITY CLASSIFICATION

DISTRIBUTION/AVAILABILITY OF REPORT

2b. DECLASSIFICATION/DOWNGRADING

Unlimited

AD-A222 024

4. PERFORMING ORGANIZATION REPORT NUMBER(S)

interim technical report #39

5. MONITORING ORGANIZATION REPORT NUMBER(S)

6a. NAME OF PERFORMING ORGANIZATION

Department of Chemistry

6b. OFFICE SYMBOL  
(if applicable)

7a. NAME OF MONITORING ORGANIZATION

Office of Naval Research

6c. ADDRESS (City, State, and ZIP Code)

Massachusetts Institute of Technology  
77 Mass. Avenue, Bldg. 6-335  
Cambridge, MA 02139

7b. ADDRESS (City, State, and ZIP Code)

Chemistry Division  
800 N. Quincy Street  
Arlington, VA 222178a. NAME OF FUNDING/SPONSORING  
ORGANIZATION

Office of Naval Research

8b. OFFICE SYMBOL  
(if applicable)

9. PROCUREMENT INSTRUMENT IDENTIFICATION NUMBER

N00014-84-K-0553

8c. ADDRESS (City, State, and ZIP Code)

Chemistry division  
800 N. Quincy Street  
Arlington, VA 22217

10. SOURCE OF FUNDING NUMBERS

PROGRAM  
ELEMENT NO.PROJECT  
NO.TASK  
NO.WORK UNIT  
ACCESSION NO.

051-579

11. TITLE (Include Security Classification)

Potential dependence of the Conductivity of Highly Oxidized Polythiophenes...

12. PERSONAL AUTHOR(S)

D. Ofer, R.M. Crooks and M.S. Wrighton

13a. TYPE OF REPORT

technical interim

13b. TIME COVERED

FROM 5/89 TO 5/90

14. DATE OF REPORT (Year, Month, Day)

5/16/90

15. PAGE COUNT

64

16. SUPPLEMENTARY NOTATION

Prepared for publication in the Journal of the American Chemical Society

17. COSATI CODES

FIELD

GROUP

SUB-GROUP

18. SUBJECT TERMS (Continue on reverse if necessary and identify by block number)

polythiophenes, polyaniline, polypyrroles, high  
conductivity

19. ABSTRACT (Continue on reverse if necessary and identify by block number)

See Attached Sheet

20. DISTRIBUTION/AVAILABILITY OF ABSTRACT

☐ UNCLASSIFIED/UNLIMITED☐ SAME AS RPT.☐ DTIC USERS

21. ABSTRACT SECURITY CLASSIFICATION

Unlimited

22a. NAME OF RESPONSIBLE INDIVIDUAL

Mark S. Wrighton

22b. TELEPHONE (Include Area Code)

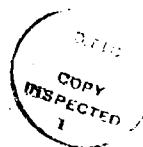
617-253-1597

22c. OFFICE SYMBOL

**Abstract**

*In situ* measurements of the relative conductivity of polythiophenes, polyaniline, and polypyrroles as a function of electrochemical potential reveal that they have finite potential dependent windows of high conductivity. The polymers studied, polyaniline and I-VI, are prepared by anodic polymerization onto microelectrode arrays of the appropriate monomer: thiophene, I, 3-methylthiophene, II, 3-phenylthiophene, III, 1-Methyl-1'-(3-thiophene-3-yl)-propyl-4,4'-bipyridinium, IV, 3,4-dimethylpyrrole, V, and N-methylpyrrole, VI. The use of liquid SO<sub>2</sub>/electrolyte medium as the electrochemical solvent makes it possible to define the window of high conductivity because it allows the polymers to be reversibly oxidized to a greater extent than has previously been achieved. The conductivities of I-IV increase by at least 10<sup>6</sup>-10<sup>9</sup> when they are oxidized from neutral to the potential of maximum conductivity, and then decrease by 10<sup>1</sup>-10<sup>4</sup> when they are further oxidized to the greatest extent possible without irreversible degradation in liquid SO<sub>2</sub>/electrolyte. Cyclic voltammetry indicates that IV is oxidized by ~0.3 electron per thiophene repeat unit at the potential of maximum conductivity, and by ~0.5 electron per repeat unit at the most positive potential accessible without irreversible degradation. Visible-near infrared absorption spectroscopy of II at the most positive potential accessible is similar to that at the potential of maximum conductivity, the spectrum having a broad peak

extending into the infrared. For thiophene-based polymers **I**, **II**, **III**, and **IV**, the maximum conductivities are approximately  $10^{-1}$ , 10,  $5 \times 10^{-2}$ , and  $5 \times 10^{-3} \Omega^{-1} \text{ cm}^{-1}$ , respectively, and the widths of the windows of high conductivity are 0.77, 0.98, 0.65, and 0.47 V, respectively. The trend for both properties is **II** > **I** > **III** > **IV**. Polyaniline undergoes large, reversible, potential dependent changes in conductivity in liquid  $\text{SO}_2$ /electrolyte in the apparent absence of a protonation/deprotonation mechanism. Conductivity increases by at least  $10^8$  upon oxidizing polyaniline from neutral to maximally conducting, and decreases by at least  $10^8$  when polyaniline is further oxidized to the point at which no faradaic current is observed in the cyclic voltammogram. Polyaniline can be taken to  $\sim +3.8$  V vs. SCE in liquid  $\text{SO}_2$ /electrolyte without irreversible degradation. Visible-near infrared spectroscopy shows that fully oxidized polyaniline absorbs only at high energy with no absorption at the low energy end of the near infrared. Potential dependent windows of high conductivity and cyclic voltammetry for pyrrole-based polymers **V** and **VI** are similar to those for thiophene-based polymers **I-IV**.



Accession For	
NTIS GRA&I	<input checked="" type="checkbox"/>
DTIC TAB	<input type="checkbox"/>
Unannounced	<input type="checkbox"/>
Justification	
By	
Distribution/	
Availability Codes	
Dist	Special and/or Special
<b>A-1</b>	

Office of Naval Research  
Contract NOOO14-84-K-0553  
Task No. 051-597  
Technical Report #39

Potential Dependence of the Conductivity of Highly Oxidized  
Polythiophenes, Polypyrroles, and Polyaniline: Finite Windows of High  
Conductivity

by

David Ofer, Richard M. Crooks, and Mark S. Wrighton

Prepared for Publication

in

Journal of the American Chemical Society

Massachusetts Institute of Technology  
Department of Chemistry  
Cambridge, MA 02139

Reproduction in whole or in part is permitted for any purpose of the  
United States Government.

This document has been approved for public release and sale; its  
distribution is unlimited.

[Prepared for publication as an article in the Journal of  
the American Chemical Society.]

**Potential Dependence of the Conductivity of Highly Oxidized  
Polythiophenes, Polypyrroles, and Polyaniline: Finite  
Windows of High Conductivity**

David Ofer, Richard M. Crooks, and Mark S. Wrighton\*

Department of Chemistry  
Massachusetts Institute of Technology  
Cambridge, Massachusetts 02139

\*Author to whom correspondence should be addressed.

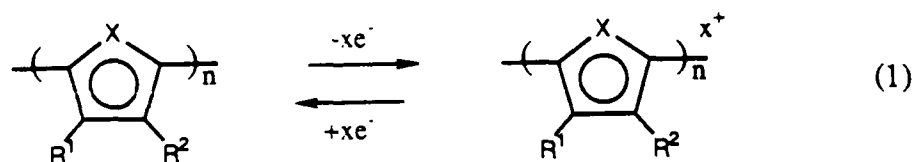
## Abstract

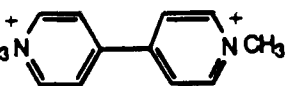
*In situ* measurements of the relative conductivity of polythiophenes, polyaniline, and polypyrroles as a function of electrochemical potential reveal that they have finite potential dependent windows of high conductivity. The polymers studied, polyaniline and **I-VI**, are prepared by anodic polymerization onto microelectrode arrays of the appropriate monomer: thiophene, **I**, 3-methylthiophene, **II**, 3-phenylthiophene, **III**, 1-Methyl-1'-(3-thiophene-3-yl)-propyl-4,4'-bipyridinium, **IV**, 3,4-dimethylpyrrole, **V**, and N-methylpyrrole, **VI**. The use of liquid SO<sub>2</sub>/electrolyte medium as the electrochemical solvent makes it possible to define the window of high conductivity because it allows the polymers to be reversibly oxidized to a greater extent than has previously been achieved. The conductivities of **I-IV** increase by at least 10<sup>6</sup>-10<sup>9</sup> when they are oxidized from neutral to the potential of maximum conductivity, and then decrease by 10<sup>1</sup>-10<sup>4</sup> when they are further oxidized to the greatest extent possible without irreversible degradation in liquid SO<sub>2</sub>/electrolyte. Cyclic voltammetry indicates that **IV** is oxidized by ~0.3 electron per thiophene repeat unit at the potential of maximum conductivity, and by ~0.5 electron per repeat unit at the most positive potential accessible without irreversible degradation. Visible-near infrared absorption spectroscopy of **II** at the most positive potential accessible is similar to that at the potential of maximum conductivity, the spectrum having a broad peak

extending into the infrared. For thiophene-based polymers **I**, **II**, **III**, and **IV**, the maximum conductivities are approximately  $10^{-1}$ , 10,  $5 \times 10^{-2}$ , and  $5 \times 10^{-3} \Omega^{-1} \text{ cm}^{-1}$ , respectively, and the widths of the windows of high conductivity are 0.77, 0.98, 0.65, and 0.47 V, respectively. The trend for both properties is **II** > **I** > **III** > **IV**.

Polyaniline undergoes large, reversible, potential dependent changes in conductivity in liquid  $\text{SO}_2$ /electrolyte in the apparent absence of a protonation/deprotonation mechanism. Conductivity increases by at least  $10^8$  upon oxidizing polyaniline from neutral to maximally conducting, and decreases by at least  $10^8$  when polyaniline is further oxidized to the point at which no faradaic current is observed in the cyclic voltammogram. Polyaniline can be taken to  $\sim +3.8$  V vs. SCE in liquid  $\text{SO}_2$ /electrolyte without irreversible degradation. Visible-near infrared spectroscopy shows that fully oxidized polyaniline absorbs only at high energy with no absorption at the low energy end of the near infrared. Potential dependent windows of high conductivity and cyclic voltammetry for pyrrole-based polymers **V** and **VI** are similar to those for thiophene-based polymers **I-IV**.

In this paper we report the potential dependence of the conductivity of thiophene-based polymers **I-IV** and pyrrole-based polymers **V** and **VI**. Our results show that all of the polymers have a finite potential window of high conductivity when they are electrochemically oxidized in low temperature  $\text{SO}_2$ /electrolyte media, equation (1). In all cases the



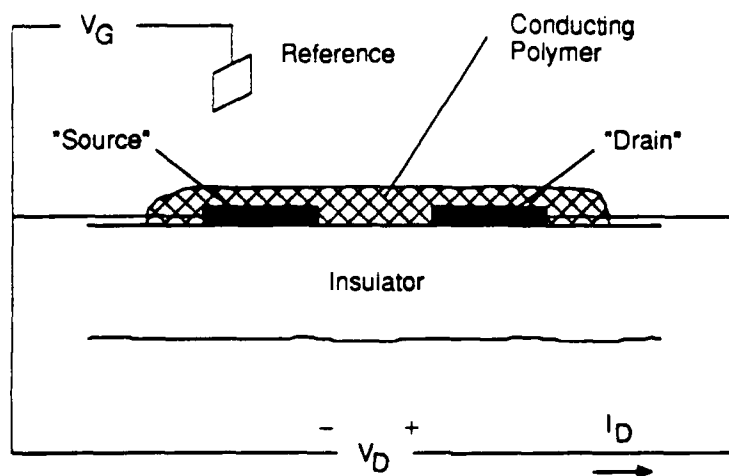
I	X=S	R <sup>1</sup> =H	R <sup>2</sup> =H
II	X=S	R <sup>1</sup> =H	R <sup>2</sup> =CH <sub>3</sub>
III	X=S	R <sup>1</sup> =H	R <sup>2</sup> =C <sub>6</sub> H <sub>5</sub>
IV	X=S	R <sup>1</sup> =H	R <sup>2</sup> =(CH <sub>2</sub> ) <sub>3</sub> N <sup>+</sup> 
V	X=NH	R <sup>1</sup> =CH <sub>3</sub>	R <sup>2</sup> =CH <sub>3</sub>
VI	X=NCH <sub>3</sub>	R <sup>1</sup> =H	R <sup>2</sup> =H

polymers show sufficiently reversible oxidation that firm conclusions can be drawn concerning the potential dependence of the conductivity. We compare the behavior of **I-VI** to that of polyaniline, which has previously been shown to have a finite potential window of high conductivity.<sup>1</sup>

Microelectrode arrays have been particularly useful as analytical tools for making *in situ* measurements of potential dependent changes in the conductivity of materials.<sup>2</sup> Arrays of closely spaced (~1  $\mu\text{m}$ ), individually



addressable, band ( $\sim 2 \mu\text{m} \times 50 \mu\text{m} \times 0.1 \mu\text{m}$  thick) microelectrodes derivatized with conducting polymers and operated in a transistor-like configuration can be used to measure the potential dependence of the conductivity of the polymer, Scheme I.<sup>1,3,4</sup> The small size of the



**SCHEME I.** Configuration of a conducting polymer-based transistor. Two microelectrodes, called source and drain, are connected with a conducting polymer and a small fixed potential,  $V_D$ , is maintained between them. At the same time, their potential versus a reference electrode,  $V_G$ , is varied, thus changing the state of charge of the polymer and therefore its conductivity. When the polymer is conducting, significant drain current,  $I_D$ , flows between the source and drain, but when the polymer is insulating negligible drain current flows.  $I_D$  is directly proportional to the conductivity of the polymer. Thus, a plot of  $I_D$  vs.  $V_G$  gives relative conductivity vs. potential.

microelectrodes and the spacing between them is advantageous for two reasons. First, as electrode area (and polymer film area and thickness) is decreased, accurate potential control can be maintained at more rapid scan rates and in more

resistive media:<sup>5</sup> measurements can be made quickly in potential regions where the polymer degrades, and/or the solvent medium can be cooled to slow degradation. Second, closely spaced microelectrodes connected with minimal quantities of conducting polymer show amplification<sup>6</sup> at the frequencies or scan rates used here:  $I_D$  is from one to four orders of magnitude larger than faradaic or gate currents, and can therefore be easily measured even at fast scan rates.

In  $\text{CH}_3\text{CN}/0.1 \text{ M } [(\text{n-Bu})_4\text{N}]\text{ClO}_4$ , **II** has very high conductivity at the most positive potential to which the polymer can be taken without irreversible chemical degradation.<sup>4</sup> Similar results have been obtained for polypyrrole.<sup>3,7</sup> In contrast, polyaniline was found to have a finite window of high conductivity bounded by the potential region over which it is durable in acidic aqueous and solid electrolyte media,<sup>1,8</sup> undergoing a transition from insulating to conducting as it is oxidized, and then becoming insulating again at the positive potential limit.

More recently we have exploited the properties of less commonly used solvent/electrolyte systems to extend the potential range of chemical durability for highly oxidized and highly reduced conducting polymers. Liquid  $\text{SO}_2$  as an electrochemical solvent has been shown to have a useful potential window with an extremely positive limit ( $\sim +4.5 \text{ V}$  vs. SCE using  $[(\text{n-Bu})_4\text{N}]\text{AsF}_6$  electrolyte),<sup>9</sup> and to be a particularly good solvent for generating highly oxidized

species without chemical degradation.<sup>10</sup> It has been reported that polyacetylene is durable to a higher extent of oxidation in liquid SO<sub>2</sub> than in propylene carbonate.<sup>11</sup> Polyaniline can be reversibly oxidized in liquid SO<sub>2</sub>,<sup>12</sup> but the extent of oxidation has not been measured. In a preliminary communication<sup>13</sup> we reported that **I** and **II** have finite potential windows of high conductivity in liquid SO<sub>2</sub>/0.1 M [(n-Bu)<sub>4</sub>N]PF<sub>6</sub>, and in this respect their behavior is closer to that of polyaniline than was previously demonstrated. Experiments in liquid NH<sub>3</sub><sup>14</sup> have revealed that **II** also has a finite potential window of high conductivity when it is electrochemically reduced. In this paper we give a full account of the previously reported oxidation of **I** and **II** and extend our work to other thiophene and pyrrole-based polymers and to polyaniline. In addition to liquid SO<sub>2</sub>, CH<sub>2</sub>Cl<sub>2</sub> has been used as an electrochemical solvent in some cases. Our findings show that a finite potential window of high conductivity is a general feature of organic conducting polymers. Moreover, the potential region of high conductivity is always associated with a region where movement of the potential is accompanied by charge or discharge of the polymer, i.e. high conductivity is found at potentials where the polymer is redox active.

High conductivity in oxidized or reduced conjugated polymers is ascribed to the movement of delocalized charges and associated structural deformations along and between polymer chains.<sup>15</sup> In this case high conductivity should

only occur when the polymer contains both charged sites and uncharged sites to which the charges can move. Indeed it has been shown that polyaniline is oxidized to an extent of approximately 0.5 electron per aniline repeat unit at the potential of its maximum conductivity, and to an extent of about 1.0 electron per repeat unit when it is most oxidized and insulating.<sup>16</sup> In this respect polyaniline is much like the segregated stack organic charge transfer salts such as those of tetracyanoquinodimethane and various electron donors, which are highly conducting only when in a "mixed valence" state of fractional charge per molecule.<sup>17</sup> Theoretical calculations suggest that, in a number of conjugated polymers, the highest occupied electronic band has a finite width with at least a large fraction of the electrons being electrochemically accessible.<sup>18,19</sup> Therefore the observation of finite potential windows of high conductivity in conjugated organic polymers is consistent with the theoretical expectation that it should be possible to oxidize them to an extent sufficient to render them non-conducting, and suggests that they bear a general similarity to organic charge transfer salts in that they are highly conducting only in "mixed valence" states of fractional charge per repeat unit. This also makes them similar to conventional redox polymers, which are defined as ones where the charges are highly localized on individual redox centers as in polyvinylferrocene<sup>20</sup> or polyviologen.<sup>21</sup> However, such systems<sup>20,21,22</sup> represent an extreme among the

electronically conducting polymers. Conductivity occurs via self-exchange processes between electronically non-interacting sites. Nonetheless, like polyaniline and the organic charge transfer salts, the "conductivity" of the conventional redox polymers is maximum when there are oxidized and reduced sites.<sup>23</sup>

## Experimental Section

**Chemicals.** 3-Methylthiophene (Aldrich) was used as received. 2,2'-Bithiophene (Aldrich) and 3-phenylthiophene<sup>24</sup> were sublimed prior to use. 1-Methyl-1'-(3-thiophene-3-yl)-propyl-4,4'-bipyridinium·2PF<sub>6</sub><sup>-</sup> was recrystallized from H<sub>2</sub>O.<sup>25</sup> 3,4-Dimethylpyrrole was used as received from Professor S.L. Buchwald<sup>26</sup> and was stored under Ar in a freezer. N-methylpyrrole (Aldrich) was distilled and stored under Ar in a refrigerator. Aniline (Aldrich) was used as received. [(n-Bu)<sub>4</sub>N]PF<sub>6</sub> was recrystallized from MeOH, dried at 120 °C and 10<sup>-2</sup> torr for 1 day, and stored under Ar. [(n-Bu)<sub>4</sub>N]AsF<sub>6</sub><sup>9</sup> was precipitated by mixing aqueous solutions of [(n-Bu)<sub>4</sub>N]Br and LiAsF<sub>6</sub>, recrystallized from acetone/water, dried at 100 °C and 10<sup>-1</sup> torr, and stored in an inert atmosphere dry box. Commercial HPLC grade CH<sub>3</sub>CN was used as received. CH<sub>2</sub>Cl<sub>2</sub> (Mallinkrodt analytical grade) was used from freshly opened bottles with experiments being run under an Ar atmosphere with Woelm activity I neutral alumina added to the CH<sub>2</sub>Cl<sub>2</sub>/electrolyte. Alternatively, the CH<sub>2</sub>Cl<sub>2</sub> was distilled from P<sub>2</sub>O<sub>5</sub> and stored under Ar with experiments being run in an inert atmosphere dry box. SO<sub>2</sub> (Matheson anhydrous 99.98 %) was bubbled through concentrated H<sub>2</sub>SO<sub>4</sub> and either (experiments with [(n-Bu)<sub>4</sub>N]PF<sub>6</sub> electrolyte) passed through Woelm activity I neutral alumina and condensed into an electrochemical cell, or (experiments with [(n-Bu)<sub>4</sub>N]AsF<sub>6</sub> electrolyte) condensed onto P<sub>2</sub>O<sub>5</sub> and distilled from the P<sub>2</sub>O<sub>5</sub> onto Woelm activity I

basic alumina.  $\text{SO}_2$  was stored over the alumina until needed, at which time it was vacuum transferred to an electrochemical cell.

**Electrochemical Cells.** For conductivity change measurements in liquid  $\text{SO}_2$ , vacuum tight single compartment cells were used.<sup>27</sup> In experiments where  $[(n\text{-Bu})_4\text{N}]\text{PF}_6$  electrolyte was used, glassware was oven dried, assembled hot, loaded with electrolyte, and evacuated to  $10^{-2}$  torr while heated to  $\sim 120^\circ\text{C}$ . Cells were opened and samples introduced under a backpressure of Ar, and then were evacuated to  $10^{-2}$  torr.  $\text{SO}_2$  was condensed and experiments were run at  $-40^\circ\text{C}$  ( $\text{CH}_3\text{CN}$  slush bath). In experiments where  $[(n\text{-Bu})_4\text{N}]\text{AsF}_6$  electrolyte was used, cells were oven dried, assembled and loaded with electrolyte inside an inert atmosphere dry box, and evacuated to a final pressure of  $10^{-5}$ - $10^{-6}$  torr at  $\sim 100^\circ\text{C}$ . Then the evacuated cell, and reference, counter, and working electrodes, were taken into the dry box, assembled, and the cell was again evacuated to  $10^{-5}$ - $10^{-6}$  torr.  $\text{SO}_2$  was condensed and experiments were run at  $-70^\circ\text{C}$  (dry ice/*i*-PrOH bath).

For *in situ* spectroelectrochemical experiments in liquid  $\text{SO}_2$ , vacuum tight cells based on a previously reported design<sup>28</sup> were used, with the optically transparent electrode (OTE) extending into a Pyrex cuvette encased in a Pyrex dewar with flat Pyrex windows. The dewar's cup contained a dry ice/*i*-PrOH mixture. An identical blank cell, containing the same liquid  $\text{SO}_2$ /electrolyte

concentration as the working cell and an underivatized CTE, was positioned in the path of the spectrometer reference beam during experiments.

**Electrodes.** Arrays of eight individually addressable Pt microelectrodes,  $\sim 50\text{ }\mu\text{m}$  long,  $\sim 0.1\text{ }\mu\text{m}$  high,  $\sim 2\text{ }\mu\text{m}$  wide, and separated from each other by  $\sim 1.2\text{ }\mu\text{m}$ , were fabricated and mounted by previously reported procedures.<sup>1,3</sup> Where noted, the microelectrodes used were  $\sim 3.6\text{ }\mu\text{m}$  wide and separated from each other by  $\sim 0.2\text{ }\mu\text{m}$ , and were fabricated by a shadow deposition technique.<sup>29</sup> Microelectrode arrays were cleaned and characterized prior to use. They were cleaned by either placing a drop of freshly mixed 3:1 concentrated  $\text{H}_2\text{SO}_4$ :30%  $\text{H}_2\text{O}_2$  directly on the array for 10 sec and then rinsing with distilled  $\text{H}_2\text{O}$  or by  $\text{O}_2$  plasma etching at  $10^{-1}$  torr and 300 W for 3 min. They were pretreated and characterized by cycling the individual microelectrodes of the array in 0.5 M  $\text{H}_2\text{SO}_4$  between +1.2 V and -0.25 V vs. SCE until well defined waves were observed in the hydrogen adsorption region.<sup>30</sup>

Optically transparent electrodes were prepared by contacting a wire to tin doped indium oxide (ITO) coated glass (Delta Technologies) with Ag epoxy and the Ag epoxy was then encapsulated in insulating epoxy. OTEs were cleaned prior to derivatization by sonicating for 10 min in acetone followed by 10 min in MeOH, and then by  $\text{O}_2$  plasma etching at  $10^{-1}$  torr and 300 W for 3 min. Pt wire or gauze counter electrodes were used and oxidized Ag wires were used as quasi-reference electrodes.



**Derivatization of Electrodes.** Microelectrodes were derivatized with thiophene and pyrrole-based polymers by anodic polymerization<sup>31,32,33</sup> of the appropriate monomer from 0.1 M solution in CH<sub>3</sub>CN/0.1 M [(n-Bu)<sub>4</sub>N]PF<sub>6</sub>. Growth of polymer could be limited to a thickness sufficient to connect microelectrodes by the following procedure. The microelectrodes that were not to be derivatized were poised at a fixed potential negative of the monomer oxidation potential. The microelectrodes that were to be derivatized were scanned positive to a potential at which monomer oxidation yielded anodic current of 2-10 mA/cm<sup>2</sup>. The microelectrodes were held at these potentials until drain current began to flow between derivatized and non-derivatized microelectrodes, indicating that the growing polymer film was beginning to connect them. At this point the polymer derivatized microelectrodes were, in the case of thiophene-based polymers, stepped negative to a potential at which the polymer was reduced to its neutral state, or, in the case of pyrrole-based polymers, stepped to a potential negative of the oxidation potential for the monomer but at which the polymer remained significantly oxidized. The devices were then electrochemically characterized in fresh CH<sub>3</sub>CN/0.1 M [(n-Bu)<sub>4</sub>N]PF<sub>6</sub> and taken out of potential control in either a neutral (polythiophenes) or oxidized (polypyrroles) state. Microelectrode arrays were derivatized with polyaniline by potential cycling as has been described previously<sup>1,34</sup> and were characterized in 0.5

M NaHSO<sub>4</sub>. Polyaniline derivatized microelectrodes were taken out of potential control at either -0.2 V vs. SCE (polymer neutral and insulating) or +0.5 V vs. SCE (polymer oxidized and conducting), rinsed repeatedly with HPLC grade H<sub>2</sub>O, and then soaked in H<sub>2</sub>O for 15 min and dried under vacuum. OTEs were derivatized by similar techniques.

**Equipment.** All electrochemical experiments were performed using a Pine Instruments RDE-4 bipotentiostat and data were recorded on a Kipp and Zonen BD91 x-y-y' recorder. Spectroscopic data were obtained using a Cary 17 UV-vis-near ir spectrophotometer.

## Results

**a. Behavior of Thiophene-Based Polymers.** Figure 1 shows cyclic voltammetry of a Pt microelectrode array derivatized with I. The electrolyte medium is liquid  $\text{SO}_2/0.1 \text{ M } [n\text{-Bu}_4\text{N}]\text{PF}_6$  at  $-40^\circ \text{ C}$ . The use of this medium allows chemically reversible oxidation to a much larger extent than in  $\text{CH}_3\text{CN}/\text{electrolyte}$ . In liquid  $\text{SO}_2$ , the oxidized Ag wire quasi-reference electrode has a potential  $\sim +0.4$ – $+0.5 \text{ V}$  vs. SCE. The cyclic voltammogram shows an oxidation wave  $\sim 1.35 \text{ V}$  vs. Ag which has not been previously observed. At the positive limit of the potential excursion the cyclic voltammogram shows increasing anodic current, but further oxidation leads to irreversible degradation of the polymer. Degradation is indicated by coulombic irreversibility (additional charge passed is not recovered when the oxidized polymer is reduced), and by the irreversible loss of conductivity of the polymer.

Figure 1 also shows the  $I_D$ - $V_G$  characteristic for the same microelectrode array operated in a transistor-like configuration. The important feature is that  $I_D$ , and therefore conductivity, significantly declines upon oxidation beyond  $\sim 0.8 \text{ V}$  vs. Ag, indicating that the polymer has a finite potential dependent window of high conductivity. This  $I_D$ - $V_G$  characteristic is scan rate independent in the range  $10^1$ – $10^3 \text{ mV/sec}$ , and it is evident that large changes in conductivity are correlated with peaks in the cyclic voltammogram. There is sweep rate independent

hysteresis in the potential dependence of conductivity: the positive and the negative sweeps of the  $I_D$ - $V_G$  trace do not show onset and decline of  $I_D$  at the same potentials, and this too correlates with hysteresis in the cyclic voltammetry. The maximum conductivity is lower on the negative sweep than on the positive sweep and the magnitudes of  $I_D$  are reproducible on subsequent scans. The difference in conductivity for the positive and negative sweeps does not, therefore, result from degradation of the polymer.

Data for arrays derivatized with **II** or **III**, Figures 2 and 3, are very similar to those for the array derivatized with **I**. The use of the low temperature  $\text{SO}_2$ /electrolyte medium allows reversible oxidation to potentials sufficiently positive to demonstrate an  $I_D$ - $V_G$  characteristic which shows a finite potential window of high conductivity with conductivity changes coinciding with cyclic voltammetry peaks. Liquid  $\text{SO}_2$  is not unique in this respect; a finite window of high conductivity can also be demonstrated for **II** in  $\text{CH}_2\text{Cl}_2$ /electrolyte, Figure 4. In  $\text{CH}_2\text{Cl}_2$ , the potential of the Ag wire quasi-reference electrode is  $\sim 0.5$  V negative of its potential in liquid  $\text{SO}_2$ . However, highly oxidized **II** is less durable in  $\text{CH}_2\text{Cl}_2$  than in liquid  $\text{SO}_2$ , with the positive potential sweep limit being dictated by the onset of rapid irreversible oxidation of the polymer and/or the solvent at the potential of the more positive anodic cyclic voltammetry peak. It is noteworthy that in  $\text{CH}_2\text{Cl}_2$  the separation between the more positive anodic and cathodic

17

cyclic voltammetry peaks for **II**, and the associated hysteresis on the positive side of the  $I_D$ - $V_G$  characteristic, is ~0.5 V, whereas in liquid  $SO_2$  the hysteresis is ~0.2 V.

There are some differences in the behaviors of **I**, **II**, and **III**, but the essential features are the same: a finite region of high conductivity in the vicinity where substantial redox behavior is found. Cyclic voltammograms for **I-III** in liquid  $SO_2$ , Figures 1-3, all indicate that the amount of charge passed when the polymers are oxidized from the neutral insulating form to maximally conducting approximately equals that passed when they are further oxidized to the positive potential limit. But it is difficult to estimate the absolute extent of oxidation per thiophene repeat unit associated with conductivity changes in **I-III**, because it is difficult to determine how much polymer has been deposited on the microelectrode arrays in the anodic polymerization process. Therefore a polymer made by electrochemical oxidation of 1-methyl-1'-(3-thiophene-3-yl)-propyl-4,4'-bipyridinium, **IV**,<sup>25</sup> has been investigated. The total amount of polymer can be determined by integrating the cyclic voltammogram for the reversible reduction of its pendant N,N'-dialkyl-4,4'-bipyridinium (viologen) redox groups, because each viologen accepts an integral number of electrons upon reduction. Thus, the integration of the two, one-electron reduction waves yields the number of thiophene repeat units on the surface. The area of the voltammogram corresponding to oxidation of the polythiophene backbone can

then be used to determine the extent of oxidation per thiophene repeat unit. Figure 5 shows the cyclic voltammogram of a Pt electrode derivatized with **IV** in  $\text{CH}_3\text{CN}/0.1 \text{ M } [(n\text{-Bu})_4\text{N}]\text{PF}_6$ . Integration of the viologen wave indicates coverage of  $6 \times 10^{-8}$  mole repeat unit per  $\text{cm}^2$ . At the positive potential limit used, the polythiophene backbone is oxidized to the extent of  $\sim 0.25$  electron per thiophene ring. Figure 6 shows cyclic voltammetry and the  $I_D$ - $V_G$  characteristic in liquid  $\text{SO}_2$  of a microelectrode array derivatized with **IV**. Comparing the voltammogram of **IV** in  $\text{SO}_2$  with that in  $\text{CH}_3\text{CN}$ , we estimate that **IV** in liquid  $\text{SO}_2$  is oxidized by  $\sim 0.25$  electron per thiophene ring at  $+0.7 \text{ V}$  vs. Ag. By integrating the voltammogram we estimate that at the anodic limit,  $+1.5 \text{ V}$ , **IV** is oxidized by  $\sim 0.5$  electron per ring, and that at the potential of maximum conductivity on the anodic sweep,  $+0.86 \text{ V}$ , **IV** is oxidized by  $\sim 0.3$  electron per ring. Our results for **IV** are thus reasonably consistent with published data for the degree of oxidation for highly conducting samples of **I** and **II** which have been measured in the  $0.15$ - $0.5$  electron per ring range by techniques including electrochemical methods,<sup>35,36,37</sup> x-ray photoelectron spectroscopy,<sup>38</sup> and elemental microanalysis.<sup>32,39</sup>

All of the thiophene-based polymers discussed so far, **I-IV**, have the same qualitative behavior: the neutral form is insulating, oxidation by  $\sim 0.3$  electron per repeat unit yields the maximum conductivity, and further oxidation yields lower conductivity. However, some important

differences exist among the four systems. The more positive cyclic voltammetry peaks for **III** and **IV**, Figures 2 and 6, are smaller than those for **I** and **II**, Figures 1 and 3. The conductivity changes associated with those peaks are also smaller for **III** and **IV**: significant  $I_D$  is evident at the positive  $V_G$  limit for **III** and **IV**, whereas for **I** and **II**,  $I_D$  returns to the baseline at the positive limit. However, Figure 6 includes a plot of steady-state resistance for **II** as a function of  $V_G$  for the same derivatized microelectrodes for which the  $I_D$ - $V_G$  data is shown. The method for measuring these resistances has been described previously.<sup>1,3,4</sup> The data show that as **II** is oxidized to 0.8 V, the resistance between adjacent microelectrodes decreases by a factor of almost  $10^8$ , whereas when it is further oxidized to 1.8 V, resistance only increases by  $10^2$ - $10^3$ . Similar results were obtained for **I**. The point is that for **I** and **II**, as well as for **III** and **IV**, the highly oxidized polymers can not be made as resistive as the neutral polymers. Resistances for transistors based on **III** and **IV** are also about  $10^{10}$ - $10^{11} \Omega$  when  $V_G$  is at the negative limit. For these polymers, resistances at the positive  $V_G$  limit are obviously relatively low, as indicated by relatively large drain currents shown in the  $I_D$ - $V_G$  characteristics.

One point regarding the data in Figure 3 needs to be addressed. The resistance measured includes the resistance of the microelectrode leads. When the polymer resistance is significantly greater than the lead resistance, the latter

is unimportant. However, when lead resistance is significant compared to that of the polymer, the  $I_D$ - $V_G$  data can be misleading. The minimum resistance of **II** is sufficiently small that the lead resistance does introduce a problem. The leads typically have a 200-250  $\Omega$  resistance per pair of Pt microelectrodes. Therefore in Figure 3, this is essentially the resistance measured when **II** is most conductive. The point is that  $I_D$  is limited by the resistance of the leads for the peak currents shown in the  $I_D$ - $V_G$  characteristic. Based on measurements of the microelectrode lead resistances and on other measurements with **II**-based transistors, we estimate that minimum polymer resistances for the device shown in Figure 3 are  $\sim 20 \Omega$ , corresponding to a maximum conductivity of  $\sim 10 \Omega^{-1} \text{ cm}^{-1}$ . Therefore the conductivity of **II** actually changes by at least  $10^9$  on the negative side of the  $I_D$ - $V_G$  peak, and by almost  $10^4$  on the positive side. If  $I_D$  were limited by the resistance of the polymer alone, and not by that of the leads, the peak  $I_D$  current would be about 10 times larger than actually observed in the  $I_D$ - $V_G$  plot. In the case of **I**, we estimate that for the device shown in Figure 1, the actual minimum polymer resistance is 250-500  $\Omega$  which would lead to a peak  $I_D$  about twice as large as that actually observed in the  $I_D$ - $V_G$  plot. In the cases of **III** and **IV**, the microelectrode lead resistance is much smaller than the polymer resistance and does not significantly limit drain currents. The important observation regarding differences



among the polythiophene systems is that the maximum conductivities and the widths of the potential windows of high conductivity both appear to follow the trend  $\text{II} > \text{I} > \text{III} > \text{IV}$ .

Polythiophenes **I-IV**, at the maximum positive potential in liquid  $\text{SO}_2$  (limited by the onset of polymer degradation), are oxidized to an extent that is significantly less than 1 electron per thiophene repeat unit, *vide supra*. Large anodic currents at the positive potential limit indicate that the highest occupied band in each polymer still has significant electron population at this potential. Therefore, the polymers may be viewed as remaining in a "mixed valence" state yielding conductivity at the positive limit several orders of magnitude higher than for the neutral polymers.

Optical absorption spectroscopy supports the conclusion that the polythiophenes are "mixed valence" at the most positive potential limits accessible. Figure 7 shows visible-near infrared absorption spectra for **II** in liquid  $\text{SO}_2$ /electrolyte at several potentials. The spectra were taken in order of increasingly positive potential, as in a positive sweep. The spectrum at  $-0.6$  V is that known for neutral **II**, while the broad spectrum at  $+0.75$  V (the potential of maximum conductivity) extends into the infrared and is similar to other spectra reported for highly conducting (oxidized) **II**.<sup>33,37,39,40</sup> At  $+1.55$  V, the most positive potential, the spectrum is quite similar to that at

+0.75 V, indicating only a small change in electronic structure compared to the change in going from the neutral to the maximally conducting oxidized state. This is consistent with the highest occupied electronic band remaining partially populated.

**b. Behavior of Polyaniline in Liquid  $\text{SO}_2$ .** The behavior of polyaniline in liquid  $\text{SO}_2$ /electrolyte, Figure 8, differs from that found for the polythiophenes. The cyclic voltammetry shows negligible faradaic current at the positive limit of potential excursion, indicating complete depopulation of the highest occupied electronic band. This, as shown by the plot of steady-state resistance vs.  $V_G$ , is accompanied by a decline in conductivity to values similar to those for neutral polyaniline.

This contrast between the thiophene based polymers and polyaniline is further defined by the differences in the spectroelectrochemistry for **II**, Figure 7, and for polyaniline, Figure 9. Figure 9 shows visible-near infrared absorption spectra of polyaniline in liquid  $\text{SO}_2$ /electrolyte at several potentials: -0.65 V where polyaniline is neutral (reduced) and insulating; +0.35 V where oxidized polyaniline has maximum conductivity; and +1.35 V where the oxidized polyaniline is very insulating. The spectra shown are similar to those that have previously been reported for polyaniline in varying degrees of oxidation and protonation.<sup>41</sup> The neutral, insulating polymer absorbs only at high energy while the highly conductive film has intense

low energy absorption trailing into the infrared, as found for **II**, Figure 7. However, in contrast to results for **II**, polyaniline shows negligible absorption in the near infrared upon oxidation to the positive potential limit. The bleaching of the near infrared absorption associated with high conductivity, together with the absence of faradaic current at the positive limit of the cyclic voltammogram, is consistent with essentially complete depopulation of the highest occupied electronic band of polyaniline.

The fact that oxidation of polyaniline to +1.35 V vs. Ag yields complete removal of electrons from the highest occupied electronic band is consistent with findings showing reversible removal of one electron per repeat unit from polyaniline.<sup>16</sup> The remarkable durability of polyaniline in liquid SO<sub>2</sub>/electrolyte allows us to address the question of whether a deeper band is electrochemically accessible by going to a more positive potential. Figure 10 shows the cyclic voltammogram and corresponding  $I_D$ - $V_G$  characteristic for polyaniline to a positive limit of 3.4 V vs. Ag. Unfortunately, the liquid SO<sub>2</sub>/electrolyte medium precludes a more positive excursion and we are unable to observe further oxidation of the polyaniline. Maintaining polyaniline in its fully oxidized state for prolonged periods does have some effect (but not an irreversible effect) on the polymer as shown by the negative scans of the Figure 10 plots. The negative scan of the cyclic voltammogram in Figure 10 shows the more positive cathodic peak at a potential negative of

that observed when polyaniline is subjected to a less positive potential, Figure 8. Figure 10 also shows that there is a decline in conductivity as reflected by the relatively lower  $I_D$  in the negative scan of the  $I_D-V_G$  characteristic compared with that in Figure 8. However, these effects are reversed upon holding polyaniline at the potential of maximum conductivity. Thus, even though polyaniline does not undergo further electrochemical oxidation beyond  $\sim 1.0$  V vs. Ag, the material is remarkably durable to  $+3.4$  V vs. Ag.

There are differences in the cyclic voltammograms for polyaniline in liquid  $\text{SO}_2$  shown in Figures 8-10 which merit some discussion. The cyclic voltammetry shown in Figure 9 resembles the voltammetry typically observed in aqueous acid media.<sup>1,42</sup> The data in Figures 8 and 10 were collected under what were probably the most rigidly anhydrous and aprotic conditions used in our experiments, there having been activated basic alumina present in the bottom of the electrochemical cell, and the electrolyte having been dried in the cell at  $100^\circ\text{C}$  and  $10^{-6}$  torr. Under less dry conditions (no alumina in the cell, electrolyte less thoroughly dried, cell not evacuated to as low a final pressure before filling with  $\text{SO}_2$ ), the cyclic voltammetry bears more resemblance to that in aqueous acid. This might be expected, given that water/ $\text{SO}_2$  solutions are known to be acidic.<sup>43</sup> However, the potential dependence of conductivity is essentially the same regardless of how dry the

SO<sub>2</sub>/electrolyte is. Indeed, the  $I_D$ - $V_G$  plot for polyaniline is similar in 0.5 M H<sub>2</sub>SO<sub>4</sub>,<sup>1</sup> liquid SO<sub>2</sub>/electrolyte, and poly(vinyl alcohol)/H<sub>3</sub>PO<sub>4</sub>·nH<sub>2</sub>O.<sup>8</sup> However, the positive potential limit in aqueous media is limited by rapid irreversible degradation beyond ~+0.8 V vs. SCE. Under the most anhydrous conditions in liquid SO<sub>2</sub>, holding polyaniline in its fully oxidized state has only slight effect on its behavior, Figure 10. Under less anhydrous conditions, holding the polymer in its fully oxidized state causes conductivity to decline more rapidly and causes the most positive cyclic voltammetry peaks to shift further negative. The magnitude of both effects is roughly in proportion to the length of time for which the polymer is held fully oxidized. But remarkably, even when these effects are relatively severe, they are slowly reversed by cycling polyaniline through its full potential range of electroactivity or by just holding it at the potential of maximum conductivity. Lastly, the behavior of polyaniline is not influenced by the oxidation state it is in when transferred to the liquid SO<sub>2</sub>/electrolyte medium. Identical responses are observed for films that are taken out of potential control in aqueous acid solutions in either the neutral (insulating) or the 50% oxidized (conducting) states, and then rinsed with pH 7 H<sub>2</sub>O. Also, final rinsings with either (CH<sub>3</sub>CH<sub>2</sub>)<sub>3</sub>N or CH<sub>3</sub>CN have no significant effect on the electrochemical response of polyaniline in liquid SO<sub>2</sub>/electrolyte.

c. **Behavior of Pyrrole-Based Polymers.** Figures 11 and 12 present data for poly(3,4-dimethylpyrrole), **V**, and poly(N-methylpyrrole), **VI**, showing that the potential dependence of their conductivity is much like that of the thiophene-based polymers. For **V** or for polypyrrole itself which are relatively easily oxidized, the liquid  $\text{SO}_2$ /electrolyte medium is not useful due to the relatively easy reduction of  $\text{SO}_2$ . Figure 11 shows characterization of **V** in  $\text{CH}_2\text{Cl}_2$ /electrolyte. The cyclic voltammogram of **V** has relatively large anodic and cathodic peaks at  $\sim 1.8$  V and  $\sim 1.2$  V, respectively. The anodic peak coincides with a decline in conductivity as the highly conducting polymer is further oxidized, and the cathodic peak coincides with a rise in conductivity as the highly oxidized polymer is reduced. The steady-state resistance of the polymer could not be measured in this potential regime because the durability of highly oxidized **V** is quite limited in  $\text{CH}_2\text{Cl}_2$ , and therefore the data shown were collected at a fast scan rate with the solution cooled to near its freezing point. In order that the polymer remain in reasonable potential equilibrium with the electrode under these conditions, a particularly thin film of polymer was used. Though not shown, polypyrrole has an electrochemical response quite similar to that for **V** in the same medium.

Figure 12 shows the characterization of **VI** in liquid  $\text{SO}_2$ /electrolyte. The more positive anodic and cathodic cyclic voltammetry peaks, at  $\sim 1.6$  V and  $\sim 1.2$  V,

respectively, are not large, and neither are the associated changes in conductivity. The conductivity of highly oxidized **VI** at the positive potential limit is not less than 20% of its maximum conductivity on the positive sweep. In addition to having very limited durability when highly oxidized, **VI** also has a low maximum conductivity and slow redox kinetics in liquid  $\text{SO}_2$ . Therefore microelectrode arrays with a smaller ( $0.2 \mu\text{m}$ ) interelectrode gap<sup>29</sup> were used in order to lessen both the amount of polymer needed to connect electrodes and the length of the conduction path through the polymer. Even so, the cyclic voltammetry and  $I_D$ - $V_G$  characteristic show a significant scan rate dependence. The width of the  $I_D$ - $V_G$  characteristic at 200 mV/sec is ~12 % less than that at 1000 mV/sec shown in Figure 12. Therefore the data in Figure 12 qualitatively demonstrate a finite potential window of high conductivity for oxidized **VI** but do not accurately show the width of the window. The pyrrole-based polymers are qualitatively similar to the thiophene-based polymers, but are generally less durable and much less durable than polyaniline. The lack of ruggedness precludes detailed studies of pyrrole-based polymers at very positive potentials. Thus, studies of optical spectral changes have not been executed.

## Discussion

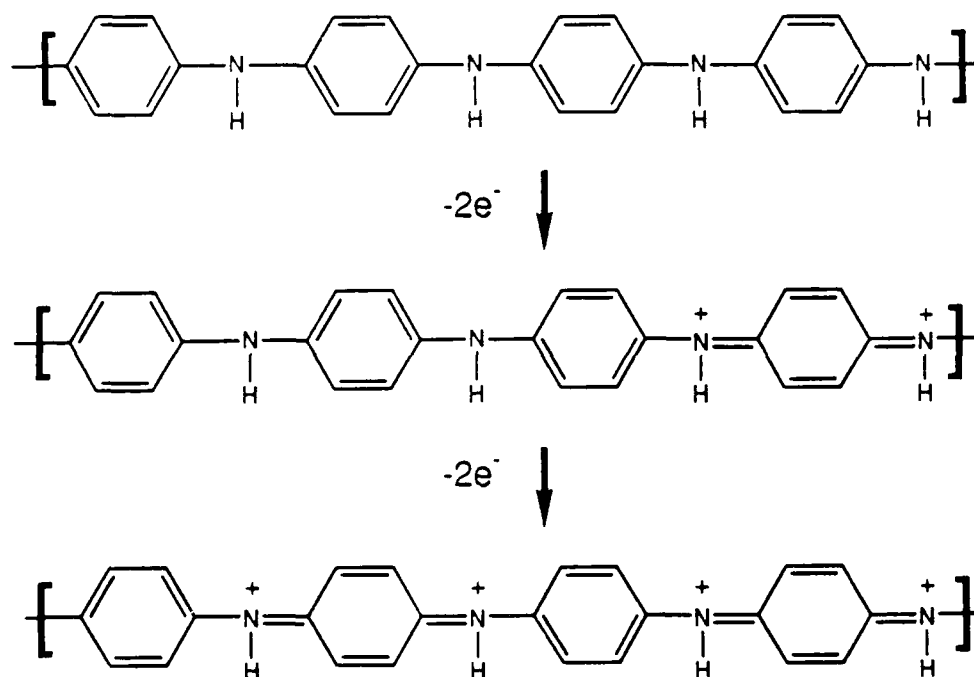
A number of general observations can be made regarding the behavior of the polymers studied. All can be demonstrated to have a finite potential window of high conductivity. Cyclic voltammetry shows that high conductivity occurs in the potential region where the polymer is redox active. This, together with optical spectroscopy, supports the conclusion that high conductivity is associated with partial depopulation of the highest occupied electronic band of the polymer, and that it is therefore associated with a "mixed valence" state of fractional charge per repeat unit of the polymer.

The ability to define the potential window of high conductivity for a polymer hinges on its durability. The durability of the polymers discussed here varies under the experimental conditions used here, but in general it is sufficient to allow reasonably accurate determination of the window of high conductivity. VI is the exception in that its electrochemical equilibration is too slow to allow it to be accurately characterized at the scan rates necessary to prevent degradation. It is noteworthy that only one of the polymers, polyaniline, is sufficiently rugged to allow its entire window of high conductivity to be studied.

The contrast between the durability of polyaniline when oxidized to the extent of 1 electron per repeat unit, and the decomposition undergone by thiophene and pyrrole-based polymers when oxidized beyond ~0.5 electron per repeat unit,







**SCHEME III.** Hypothetical structures of polyaniline at various points in its redox cycle in liquid SO<sub>2</sub>. Top: neutral and insulating. Middle: oxidized to 0.5 electron per repeat unit and highly conducting. Bottom: oxidized to 1 electron per repeat unit and insulating.

In fact it has been shown that in the protonated conducting form of polyaniline, Scheme III-middle, much of the charge resides on nitrogen atoms.<sup>46</sup> The known stability of the tetramethylphenylenediamine dication<sup>47</sup> gives reason to expect that the structure shown at the bottom of Scheme III might be stable under appropriate conditions.

Scheme III is in fact a reasonable representation of the redox cycle of polyaniline in liquid SO<sub>2</sub>/electrolyte

under sufficiently anhydrous conditions. Whereas mechanisms for the redox behavior in aqueous acid emphasize protonation and deprotonation,<sup>42</sup> we judge that protonation/deprotonation does not play a role in liquid SO<sub>2</sub>. SO<sub>2</sub> is known to be less basic than ethylene in the gas phase,<sup>48</sup> and the anions of the electrolytes we have used are also extremely weak bases.<sup>49</sup> Therefore it is reasonable to assume that fully oxidized polyaniline, Scheme III-bottom, remains fully protonated.

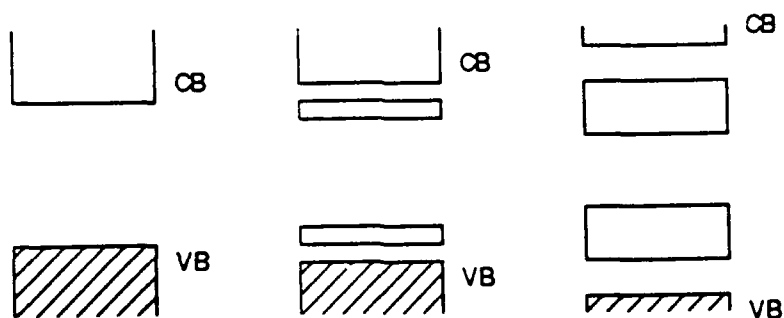
The thiophene-based polymers appear to follow a trend in which the higher the conductivity of the polymer, the wider its potential window of high conductivity. It is reasonable that these should be related, because the bandwidth of the highest occupied electronic band is a measure of delocalization in the system and should to some extent be correlated with both the charge carrier mobility,<sup>18</sup> and the width of the potential region over which the band can be depopulated. However, the band structure changes as the polymer is oxidized, and it may change in different ways for different polymers. This may be why such a trend is evident for thiophene-based polymers but not for pyrrole-based polymers.

For all the polymers studied, the conductivity changes on the positive side of the  $I_D$ - $V_G$  characteristic are accompanied by cyclic voltammetry peaks. That is, an anodic peak in the voltammogram is associated with decline in conductivity when the oxidized, highly conducting, polymer

is further oxidized, and a cathodic peak in the voltammogram is associated with increase in conductivity when the less conducting, highly oxidized, polymer is reduced. In general, it appears that the larger the changes in conductivity are, the larger the voltammetric peaks. This might be expected because changes in the conductivity of the polymer are associated with changes in the extent of delocalization of the highest energy electrons in the polymer. The more highly conducting the polymer is, the more delocalized the highest energy electrons should be and the greater the extent to which removal of any one electron lowers the energies of the others. In this state, the polymer should behave as a metal in the sense of its having a broad potential region of continuous charging. However, as conductivity declines and the highest energy electrons become more localized, the redox behavior of the polymer should approach that of an ensemble of noninteracting redox units as in conventional redox polymers like polyvinylferrocene. Under such circumstances, removal of any one of the highest energy electrons should have little effect on energies of the others, and the voltammogram should have a peak as a large number of non-interacting electrons with the same energy are removed at once.

All the polymers have cyclic voltammograms and  $I_D$ - $V_G$  plots showing significant hysteresis. The hysteresis is typically greater on the positive side of the potential of maximum conductivity than on the negative side. Hysteresis

in all the potential dependent properties of conducting polymers has been explained as the result of changes in polymer structure which cause excess charge to reside in new electronic levels located in the band gap.<sup>35,50</sup> Therefore charge is injected at potentials corresponding to the band edges (top of the valence band for oxidation of neutral polymers, bottom of the conduction band for reduction of neutral polymers), but is neutralized at potentials corresponding to the new levels located in the gap. Hysteresis in the potential dependent properties of an oxidized conducting polymer can then be a measure of the energy gap between the top of the valence band and the bottom of the lowest band in the gap when the polymer is oxidized to some given extent. Our data suggests that,



**SCHEME IV.** Hypothetical evolution of band structure upon oxidation of a polyaromatic conducting polymer. Left: neutral polymer with filled valence band, VB, and empty conduction band, CB. Middle: band structure at relatively low extent of oxidation. Valence band remains full and holes are accommodated in new bands which grow in the gap. Right: band structure at higher extent of oxidation. More states are added to bands in the gap while valence and conduction bands shrink.

as illustrated in Scheme IV, this energy gap, and therefore hysteresis, increase as the polymer is oxidized to a greater extent. Such an evolution of band structure upon oxidation has been calculated for polypyrrole.<sup>45</sup> A widening of the energy gap between the upper edge of the occupied valence band and the lower edge of the bands in the gap may be due to narrowing of the bands associated with the increased localization of charge as the highly oxidized polymer becomes less conducting. Spectroscopic absorption edges in the infrared corresponding to this energy gap have been reported for a number of oxidized conducting thiophene-based polymers<sup>39,51</sup> and for polyaniline.<sup>52</sup> Studies of infrared spectroelectrochemistry of conducting polymers in liquid SO<sub>2</sub>/electrolyte are in progress.

The  $I_D$ - $V_G$  characteristics of the polymers studied show higher maximum  $I_D$ , and therefore higher maximum conductivity, for the positive sweep than for the negative sweep. This may result from the overcoming of a kinetic barrier to charge localization within the polymer during the oxidation process. As the polymer becomes highly oxidized, coulombic repulsions could drive the polymer chains to adopt conformations in which discrete segments stabilize more localized charges, and these segments are then less involved in conduction upon reduction of the oxidized polymer.

Recent work reporting that slight changes in solvent polarity can significantly influence the extent of spin pairing in oxidized soluble poly(3-hexylthiophene),<sup>53</sup>

suggests that intrachain coulombic repulsions, and their screening by solvent and electrolyte reorganization, can play a large role in the dynamics of oxidation and charge distribution in conducting polymers. It might be expected that the effects of coulombic repulsions between polymer charge sites and their screening by solvent/electrolyte will increase as the extent of oxidation of a conducting polymer is increased. Such effects might be particularly significant in the far positive potential region, where the decline of polymer conductivity and the increase of charge localization may in part be due to a higher density of charge in the polymer. This may be relevant to the differences between the potential dependent characteristics of **II** in liquid  $\text{SO}_2$  and in  $\text{CH}_2\text{Cl}_2$ , Figures 3 and 4. On the negative side of the  $I_D$ - $V_G$  characteristic, the potential dependent behavior of **II** in  $\text{CH}_2\text{Cl}_2$  is similar to that in  $\text{SO}_2$ . This would be consistent with the expectation that the relative effects of different solvents in screening intrapolymer coulombic repulsions would be less significant at lower charge densities. However, in the more positive potential region where the polymer has a higher density of charge, the hysteresis observed in the cyclic voltammograms and  $I_D$ - $V_G$  characteristics is very different for the two solvent systems. This difference should then be an indication of differences in the evolution of the band structure as **II** is oxidized in the different solvent systems, Scheme IV.

In summary, the observation of a finite potential window of high conductivity for oxidized polythiophenes and polypyrroles, as was previously found for polyaniline, suggests that this is a general feature of conducting organic conjugated polymers, and that high conductivity in these systems is associated with "mixed valence" states of fractional charge per repeat unit. The use of appropriate solvent/electrolyte systems which extend the potential regime in which conducting polymers can be investigated reveals characteristic effects which should aid in developing a better understanding of their behavior. The use of microelectrode arrays to measure potential dependent changes in conductivity allows such measurements to be made rapidly in potential regimes where the polymers may have very limited durability.

**Acknowledgements.** We thank the Office of Naval Research, the Defense Advanced Research Projects Agency, and the National Science Foundation through the M.I.T. Materials Research Laboratory for partial support of this research. We thank Professor Robert J. Silbey for several valuable discussions and we thank Dr. Timothy M. Miller for providing us with 3-phenylthiophene, Professor Stephen L. Buchwald for providing us with 3,4-dimethylpyrrole, and Dr. Ching-Fong Shu for providing us with 1-Methyl-1'-(3-thiophene-3-yl)-propyl-4,4'-bipyridinium $\cdot$ 2PF<sub>6</sub><sup>-</sup>.



## References

1. Paul, E.W.; Ricco, A.J.; Wrighton, M.S. *J. Phys. Chem.* **1985**, *89*, 1441.
2. Natan, M.J.; Wrighton, M.S. in *Progress in Inorganic Chemistry*; Lippard, S.J., Ed.; John Wiley and Sons: New York, 1989; V 37.
3. Kittlesen, G.P.; White, H.S.; Wrighton, M.S. *J. Am. Chem. Soc.* **1984**, *106*, 7389.
4. Thackeray, J.W.; White, H.S.; Wrighton, M.S. *J. Phys. Chem.* **1985**, *89*, 5133.
5. Wightman, R.M. *Science* **1988**, *240*, 415.
6. Lofton, E.P.; Thackeray, J.W.; Wrighton, M.S. *J. Phys. Chem.* **1986**, *90*, 6080.
7. Feldman, B.J.; Burgmayer, P.; Murray, R.W. *J. Am. Chem. Soc.* **1985**, *107*, 872.
8. Chao, S.; Wrighton, M.S. *J. Am. Chem. Soc.* **1987**, *109*, 6627.
9. Garcia, E.; Kwak, J.; Bard, A.J. *Inorg. Chem.* **1988**, *27*, 4377.
10. (a) Miller, L.L.; Mayeda, E.A. *J. Am. Chem. Soc.* **1970**, *92*, 5218. (b) Tinker, L.A.; Bard, A.J. *J. Am. Chem. Soc.* **1979**, *101*, 2316.
11. Heinze, J.; Hinkelmann, K.; Dietrich, M.; Mortensen, J. *Ber. Bunsenges. Phys. Chem.* **1985**, *89*, 1225.
12. Heinze, J.; Mortensen, J.; Hinkelmann, K. *Synth. Met.* **1987**, *21*, 209.

13. Ofer, D.; Wrighton, M.S. *J. Am. Chem. Soc.* **1988**, 110, 4467.
14. Crooks, R.M.; Chyan, O.M.R.; Wrighton, M.S. *Chem. of Materials* **1989**, 1, 2.
15. Chance, R.R.; Boudreux, D.S.; Brédas, J.L.; Silbey, R. in *Handbook of Conducting Polymers*; Skotheim, T.A., Ed.; Marcel Dekker: New York, 1986; Ch 24.
16. Orata D.; Buttry, D.A. *J. Am. Chem. Soc.* **1987**, 109, 3574.
17. (a) Torrance, J.B. *Accts. Chem. Res.* **1979**, 12, 79. (b) Torrance, J.B. *Mol. Cryst. Liq. Cryst.* **1985**, 126, 55. (c) Ward, M.D. in *Electroanalytical Chemistry: A Series of Advances*; Bard, A.J., Ed.; Marcel Dekker: New York, 1989; V 16.
18. Brédas, J.L.; Elsenbaumer, R.L.; Chance, R.R.; Silbey, R. *J. Chem. Phys.* **1983**, 78, 5656.
19. (a) Boudreaux, D.S.; Chance, R.R.; Wolf, J.F.; Shacklette, L.W.; Brédas, J.L.; Thémans, B.; André, J.M.; Silbey, R. *J. Chem. Phys.* **1986**, 85, 4584. (b) Bakhshi, A.K.; Ladik, J.; Seel, M. *Phys. Rev. B* **1987**, 35, 704. (c) Statsfröm, S.; Brédas, J.L. *Mol. Cryst. Liq. Cryst.* **1988**, 160, 405.
20. (a) Smith, T.W.; Kuder, J.E.; Wychik, D. *J. Polym. Sci.* **1976**, 14, 2433. (b) Merz, A.; Bard, A.J. *J. Am. Chem. Soc.* **1978**, 100, 3222. (c) Nowak, R.; Schultz, F.A.; Umaña, M.; Abruña, H.; Murray, R.W. *J. Electroanal. Chem.* **1978**, 94, 219.

21. (a) Bookbinder, D.C.; Wrighton, M.S. *J. Am. Chem. Soc.* **1980**, *102*, 5123. (b) Abruña, H.D.; Bard, A.J. *J. Am. Chem. Soc.* **1981**, *103*, 6898. (c) Killman, K.W.; Murray, R.W. *J. Electroanal. Chem.* **1982**, *133*, 211.
22. (a) Van De Mark, M.R.; Miller, L.L. *J. Am. Chem. Soc.* **1978**, *100*, 3223. (b) Oyama, N.; Anson F.C. *J. Am. Chem. Soc.* **1979**, *101*, 739. (c) Oyama, N.; Anson, F.C. *J. Electrochem. Soc.* **1980**, *127*, 247.
23. (a) Kaufman, F.B.; Schroeder, A.H.; Engler, E.M.; Kramer, S.R.; Chambers, J.Q. *J. Am. Chem. Soc.* **1980**, *102*, 483. (b) Daum, P.; Lenhard, J.R.; Rolison, D.; Murray, R.W. *J. Am. Chem. Soc.* **1980**, *102*, 4649. (c) Pickup, P.G.; Murray, R.W. *J. Am. Chem. Soc.* **1983**, *105*, 4510.
24. Tamao, K.; Kodama, S.; Nakajima, I.; Kumada, M.; Minato, A.; Suzuki, K. *Tetrahedron* **1982**, *38*, 3347.
25. Shu, C.F.; Wrighton, M.S. in *ACS Symposium Series*, No 378, "Electrochemical Surface Science: Molecular Phenomena at Electrode Surfaces"; Soriaga, M.P., Ed.; American Chemical Society: Washington, 1988.
26. Buchwald, S.L.; Wannamaker, M.W.; Watson, B.T. *J. Am. Chem. Soc.* **1989**, *111*, 776.
27. Bard, A.J.; Faulkner, L.R. *Electrochemical Methods*; Marcel Dekker: New York, 1980; p 25.
28. Gaudiello, J.G.; Bradley, P.G.; Norton, K.A.; Woodruff, W.H.; Bard, A.J. *Inorg. Chem.* **1984**, *23*, 3.
29. Jones, E.T.T.; Chyan, O.M.; Wrighton, M.S. *J. Am. Chem.*

- Soc. **1987**, 109, 5526.
30. Breiter, M.; Böld, W. *Electrochim. Acta* **1961**, 5, 145.
  31. (a) Diaz, A.F.; Kanazawa, K.K.; Gardini, G.P. *J. Chem. Soc. Chem. Commun.* **1979**, 854. (b) Kanazawa, K.K.; Diaz, A.F.; Geiss, R.H.; Gill W.D.; Kwak, J.F.; Logan, J.A.; Rabolt, J.F.; Street, G.B. *J. Chem. Soc. Chem. Commun.* **1979**, 653. (c) Waltman, R.J.; Bargon, J.; Diaz, A.F. *J. Phys. Chem.* **1983**, 87, 1459.
  32. Tourillon, G.; Garnier, F. *J. Electroanal. Chem.* **1982**, 135, 173.
  33. Tourillon, G.; Garnier, F. *J. Electroanal. Chem.* **1983**, 148, 299.
  34. Diaz, A.F.; Logan, J.A. *J. Electroanal. Chem.* **1980**, 111, 111.
  35. Chung, T.-C.; Kaufman, J.H.; Heeger, A.J.; Wudl, F. *Phys. Rev. B* **1984**, 30, 702.
  36. Colaneri, N.; Nowak, M.; Spiegel, D.; Hotta, S.; Heeger, A.J. *Phys. Rev. B* **1987**, 36, 7964.
  37. Nagatomo, T.; Omoto, O. *J. Electrochem. Soc.* **1988**, 135, 2124.
  38. Jugnet, Y.; Tourillon, G.; Duc, T.M. *Phys. Rev. Lett.* **1986**, 56, 1862.
  39. Tourillon, G.; Garnier, F. *J. Phys. Chem.* **1983**, 87, 2289.
  40. (a) Sato, M.; Tanaka, S.; Keeriyama, K. *Synth. Met.* **1986**, 14, 279. (b) Hoier, S.N.; Ginley, D.S.; Park, S.-M. *J. Electrochem. Soc.* **1988**, 135, 91. (c) Kaneto,

- K.; Hayashi, S.; Yoshino, K. *J. Phys. Soc. Jpn.* **1988**, 57, 1119. (d) Patil, A.O.; Heeger, A.J.; Wudl, F. *Chem. Rev.* **1988**, 88, 183.
41. (a) Kobayashi, T.; Yonyama, H.; Tamura, H. *J. Electroanal. Chem.* **1984**, 161, 419. (b) Statsfröm, S.; Brédas, J.L.; Epstein, A.J.; Woo, H.S.; Tanner, D.B.; Huang, W.S.; MacDiarmid, A.G. *Phys. Rev. Lett.* **1987**, 59, 1464. (c) Epstein, A.J.; Ginder, J.M.; Zuo, F.; Bigelow, R.W.; Woo, H.S.; Tanner, D.B.; Richter, A.F.; Huang, W.S.; MacDiarmid, A.G. *Synth. Met.* **1987**, 18, 303. (d) Shacklette, L.W.; Wolf, J.F.; Gould, S.; Baughman, R.H. *J. Chem. Phys.* **1988**, 88, 3955. (e) Kim, Y.H.; Foster, C.; Chiang, J.; Heeger, A.J. *Synth. Met.* **1988**, 26, 45. (f) Ohsawa, T.; Kabata, T.; Kimura, O.; Yoshino, K. *Synth. Met.* **1989**, 29, E203.
42. Huang, W.-S.; Humphrey, B.D.; MacDiarmid, A.G. *J. Chem. Soc., Faraday Trans. 1* **1986**, 82, 2385.
43. Cotton, F.A.; Wilkinson, G. *Advanced Inorganic Chemistry*; John Wiley and Sons: New York, 1980; p 532.
44. (a) Brédas, J.L.; Chance, R.R.; Silbey, R. *Mol. Cryst. Liq. Cryst.* **1981**, 77, 319. (b) Brédas, J.L.; Thémans, B.; Fripiat, J.G.; André, J.M.; Chance, R.R. *Phys. Rev. B* **1984**, 29, 6761.
45. Brédas, J.L.; Street, G.B. *Acc. Chem. Res.* **1985**, 18, 309.
46. Kaplan, S.; Conwell, E.M.; Richter, A.F.; MacDiarmid, A.G. *J. Am. Chem. Soc.* **1988**, 110, 7647.

47. Yao, T.; Musha, S.; Munemori, M. *Chem. Lett.* **1974**, 939.
48. Collyer, S.M.; McMahon, T.B. *J. Phys. Chem.* **1983**, 87, 909.
49. Gordon, A.J.; Ford, R.A. *The Chemist's Companion*; John Wiley and Sons: New York, 1976; p 60.
50. Kaufman, J.H.; Kaufer, J.W.; Heeger, A.J.; Kaner, R.; MacDiarmid, A.G. *Phys. Rev. B* **1982**, 26, 2327.
51. Gustafsson, G.; Inganäs, O.; Nilsson, J.O.; Liedberg, B. *Synth. Met.* **1988**, 26, 297.
52. (a) Sariciftci, N.S.; Bartonek, M.; Kuzmany, H.; Neugebauer, H.; Neckel, A. *Synth. Met.* **1989**, 29, E193.  
(b) Neugebauer, H.; Neckel, A.; Sariciftci, N.S.; Kuzmany, H. *Synth. Met.* **1989**, 29, E185.
53. Nowak, M.J.; Spiegel, D.; Hotta, S.; Heeger, A.J.; Pincus, P.A. *Macromolecules* **1989**, 22, 2917.

### Figure Captions

**Figure 1.** Top: cyclic voltammetry of **I** connecting three adjacent Pt microelectrodes in  $\text{SO}_2/0.1 \text{ M } [(n\text{-Bu})_4\text{N}]\text{PF}_6$  at  $-40^\circ\text{C}$ . Integration of the voltammogram indicates reversible removal of  $7 \times 10^{-7}$  mole electrons per  $\text{cm}^2$  of area covered by polymer. Bottom:  $I_D$ - $V_G$  characteristic in the same medium for an adjacent pair of the microelectrodes connected with **I** for which cyclic voltammetry is shown. Maximum conductivity on the positive sweep is  $\sim 10^{-1} \Omega^{-1} \text{ cm}^{-1}$  and the window in which conductivity is at least 20% of maximum is 0.77 V wide.

**Figure 2.** Top: cyclic voltammetry of **III** connecting two adjacent Pt microelectrodes in  $\text{SO}_2/0.1 \text{ M } [(n\text{-Bu})_4\text{N}]\text{AsF}_6$  at  $-70^\circ\text{C}$ . Integration of the voltammogram indicates reversible removal of  $1 \times 10^{-7}$  mole electrons per  $\text{cm}^2$  of area covered by polymer. Bottom:  $I_D$ - $V_G$  characteristic in the same medium for the same pair of derivatized microelectrodes. Maximum conductivity on the positive sweep is  $\sim 5 \times 10^{-2} \Omega^{-1} \text{ cm}^{-1}$  and the window in which conductivity is at least 20% of maximum is 0.65 V wide.

**Figure 3.** Top: cyclic voltammetry of **II** connecting three adjacent Pt microelectrodes in  $\text{SO}_2/0.1 \text{ M } [(n\text{-Bu})_4\text{N}]\text{PF}_6$  at  $-40^\circ\text{C}$ . Integration of the voltammogram indicates reversible removal of  $9 \times 10^{-8}$  mole electrons per  $\text{cm}^2$  of

area covered by polymer. Middle:  $I_D-V_G$  characteristic in the same medium for an adjacent pair of microelectrodes for which cyclic voltammetry is shown. Maximum conductivity on the positive sweep is  $\sim 10 \Omega^{-1} \text{ cm}^{-1}$  and the window in which conductivity is at least 20% of maximum is 0.98 V wide. Bottom: steady-state resistance as a function of  $V_G$  for the same pair of microelectrodes for which the  $I_D-V_G$  characteristic is shown.

**Figure 4.** Top: cyclic voltammetry of **II** connecting six adjacent Au microelectrodes in  $\text{CH}_2\text{Cl}_2/0.1 \text{ M } [(n\text{-Bu})_4\text{N}]\text{PF}_6$  at  $25^\circ\text{C}$ . Integration of the voltammogram indicates reversible removal of  $8 \times 10^{-8}$  mole electrons per  $\text{cm}^2$  of area covered by polymer. Bottom:  $I_D-V_G$  characteristic in the same medium for an adjacent pair of the microelectrodes for which cyclic voltammetry is shown.

**Figure 5.** Cyclic voltammetry of **IV** on a 0.5 mm Pt disc electrode in  $\text{CH}_3\text{CN}/0.1 \text{ M } [(n\text{-Bu})_4\text{N}]\text{PF}_6$  at  $25^\circ\text{C}$ .

**Figure 6.** Top: cyclic voltammetry of **IV** connecting six adjacent Pt microelectrodes in  $\text{SO}_2/0.1 \text{ M } [(n\text{-Bu})_4\text{N}]\text{PF}_6$  at  $-40^\circ\text{C}$ . Assuming oxidation by  $\sim 0.25$  electron per thiophene ring at +0.6 V, integration of the voltammogram indicates  $3 \times 10^{-7}$  mole repeat units per  $\text{cm}^2$  of area covered by polymer. Bottom:  $I_D-V_G$  characteristic in the same medium for the six microelectrodes in an interdigitated



configuration (drain electrodes 2, 4, and 6 are offset 25 mV =  $V_D$  from source electrodes 1, 3, and 5). Maximum conductivity on the positive sweep is  $\sim 5 \times 10^{-3} \Omega^{-1} \text{ cm}^{-1}$  and the window in which conductivity is at least 20% of maximum is 0.47 V wide.

**Figure 7.** Vis-NIR spectroelectrochemistry for **II** on ITO in  $\text{SO}_2/0.2 \text{ M } [(n\text{-Bu})_4\text{N}]\text{AsF}_6$  at  $-70^\circ\text{C}$ . Inset: cyclic voltammetry of the same electrode in the spectroelectrochemical cell. Integration of the voltammogram indicates reversible removal of  $2 \times 10^{-7}$  mole electrons per  $\text{cm}^2$  of area covered by polymer.

**Figure 8.** Top: cyclic voltammetry of polyaniline connecting two adjacent Pt microelectrodes in  $\text{SO}_2/0.1 \text{ M } [(n\text{-Bu})_4\text{N}]\text{AsF}_6$  over activity I basic alumina at  $-70^\circ\text{C}$ . Integration of the voltammogram indicates  $1.2 \times 10^{-7}$  mole repeat units per  $\text{cm}^2$  of area covered by polymer. Middle:  $I_D$ - $V_G$  characteristic in the same medium for the same pair of derivatized microelectrodes. Maximum conductivity on the positive sweep is  $\sim 1 \Omega^{-1} \text{ cm}^{-1}$  and the window in which conductivity is at least 20% of maximum is 0.6 V wide. Bottom: steady-state resistance as a function of  $V_G$  for the same pair of derivatized microelectrodes.

**Figure 9.** Vis-NIR spectroelectrochemistry for polyaniline on ITO in  $\text{SO}_2/0.2 \text{ M } [(n\text{-Bu})_4\text{N}]\text{AsF}_6$  at  $-70^\circ\text{C}$ . Inset: cyclic

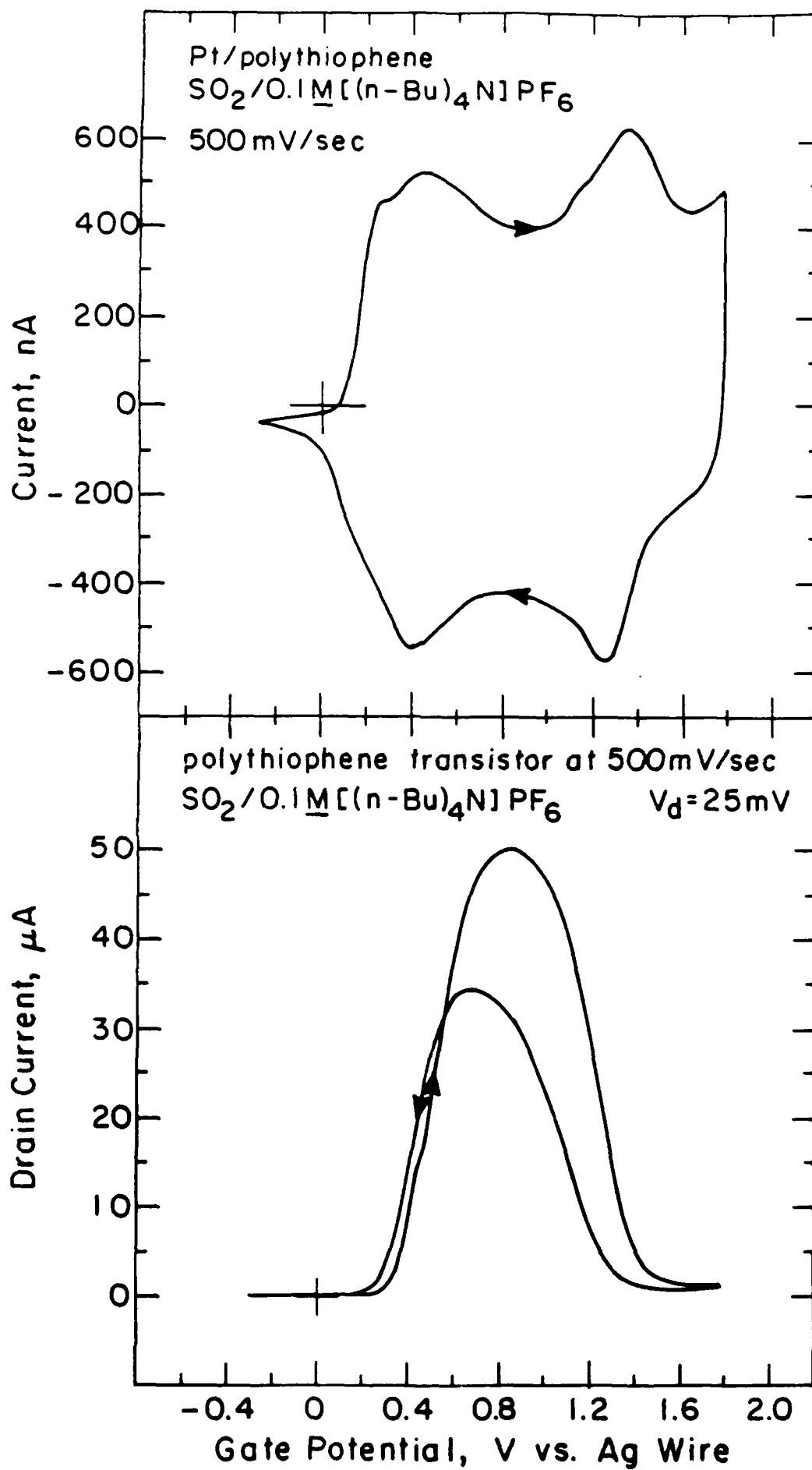
voltammetry of the same electrode in the spectroelectrochemical cell. Integration of the voltammogram indicates  $3.4 \times 10^{-7}$  mole repeat units per  $\text{cm}^2$  of area covered by polymer.

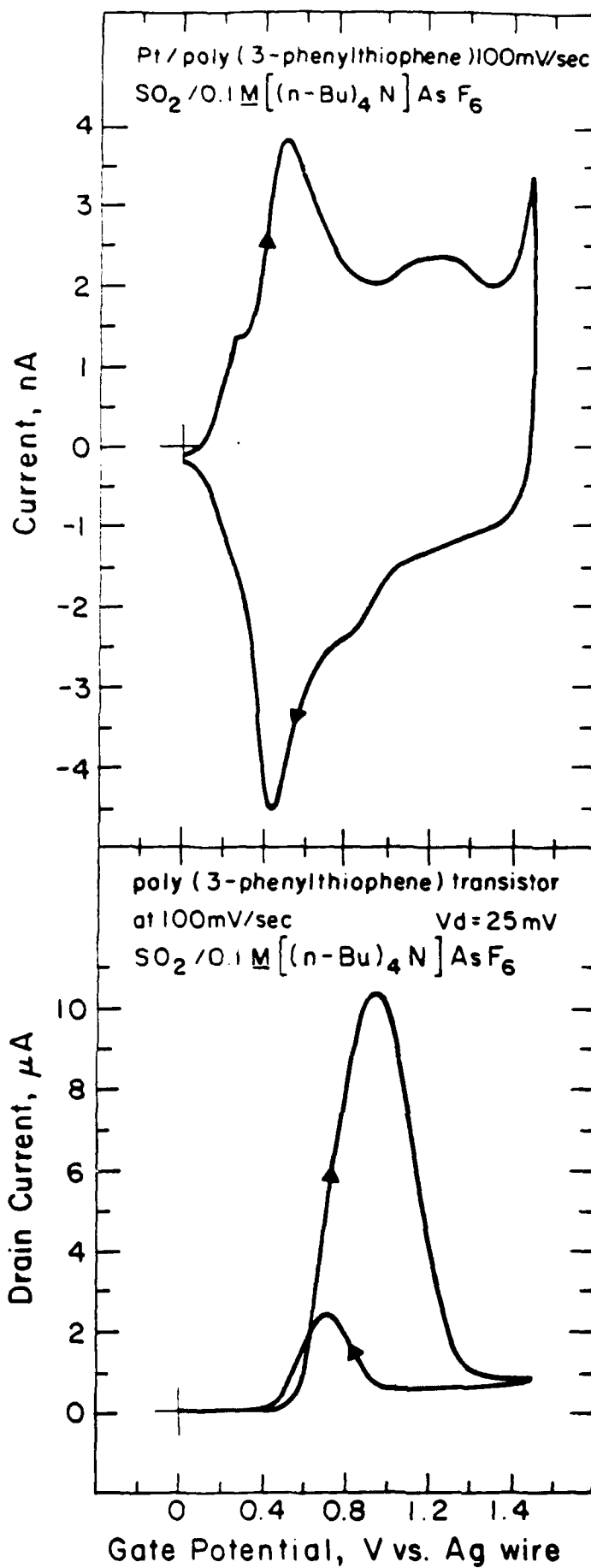
**Figure 10.** Top: cyclic voltammetry of polyaniline connecting two adjacent Pt microelectrodes in  $\text{SO}_2/0.1 \text{ M } [(n\text{-Bu})_4\text{N}]\text{AsF}_6$  over activity I basic alumina at  $-70^\circ\text{C}$ . Integration of the voltammogram indicates  $9.3 \times 10^{-8}$  mole repeat units per  $\text{cm}^2$  of area covered by polymer. Middle:  $I_D$ - $V_G$  characteristic in the same medium for the same pair of derivatized microelectrodes.

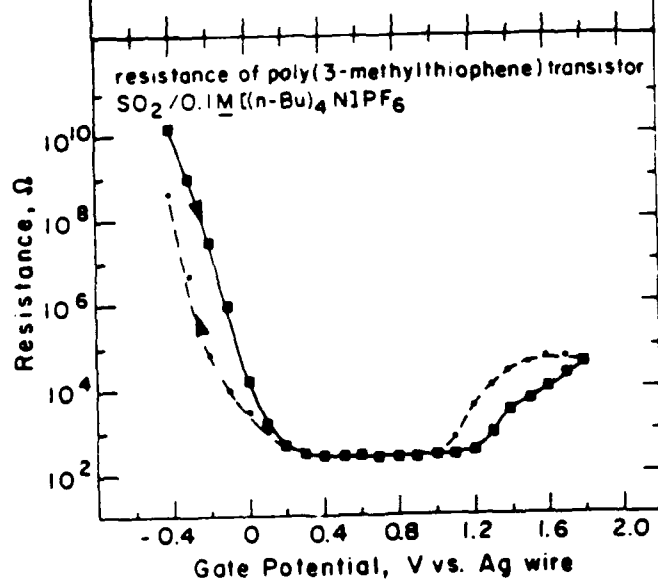
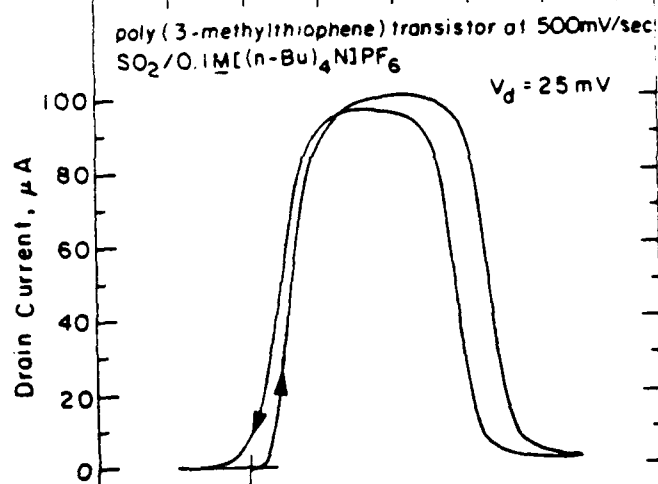
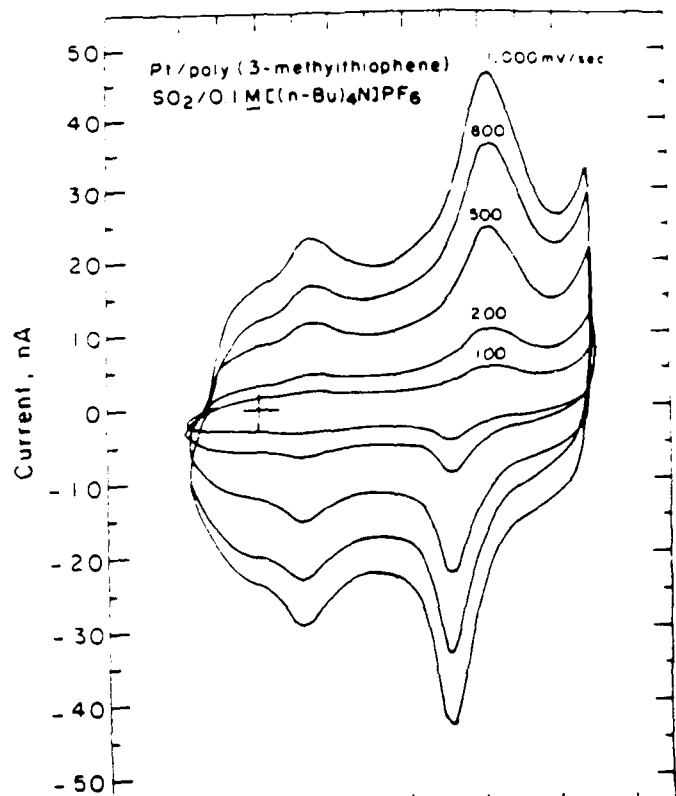
**Figure 11.** Top: cyclic voltammetry of **V** connecting two adjacent Pt microelectrodes in  $\text{CH}_2\text{Cl}_2/0.1 \text{ M } [(n\text{-Bu})_4\text{N}]\text{PF}_6$  at  $-75^\circ\text{C}$ . Integration of the voltammogram indicates reversible removal of  $2 \times 10^{-8}$  mole electrons per  $\text{cm}^2$  of area covered by polymer. Bottom:  $I_D$ - $V_G$  characteristic in the same medium for the same pair of derivatized microelectrodes. Maximum conductivity on the positive sweep is  $\sim 5 \times 10^{-1} \Omega^{-1} \text{ cm}^{-1}$  and the window in which conductivity is at least 20% of maximum is 1.2 V wide.

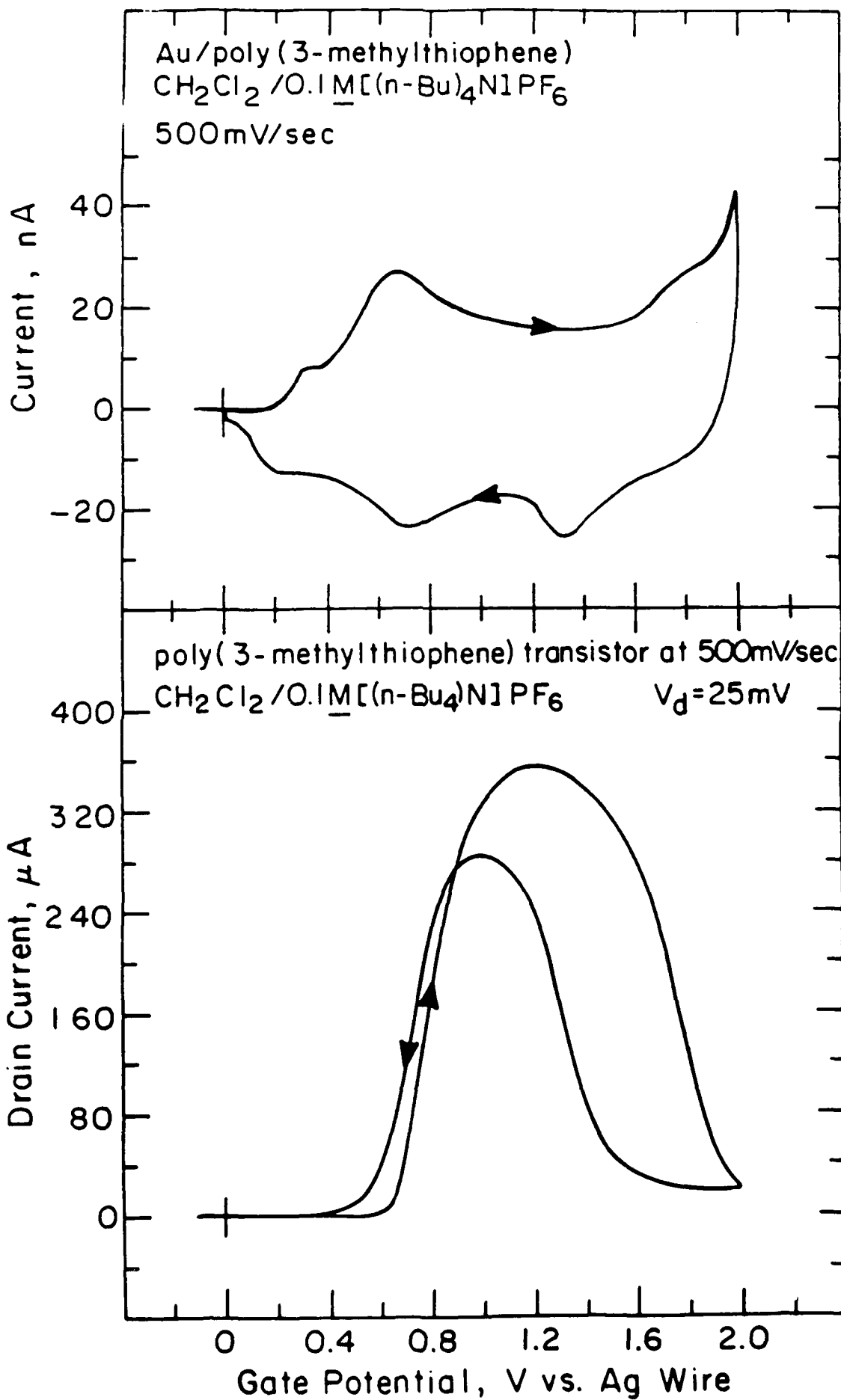
**Figure 12.** Top: cyclic voltammetry, in  $\text{SO}_2/0.1 \text{ M } [(n\text{-Bu})_4\text{N}]\text{AsF}_6$  at  $-70^\circ\text{C}$ , of **VI** connecting two adjacent Pt microelectrodes having an interelectrode gap of 200 nm. Integration of the voltammogram indicates reversible removal

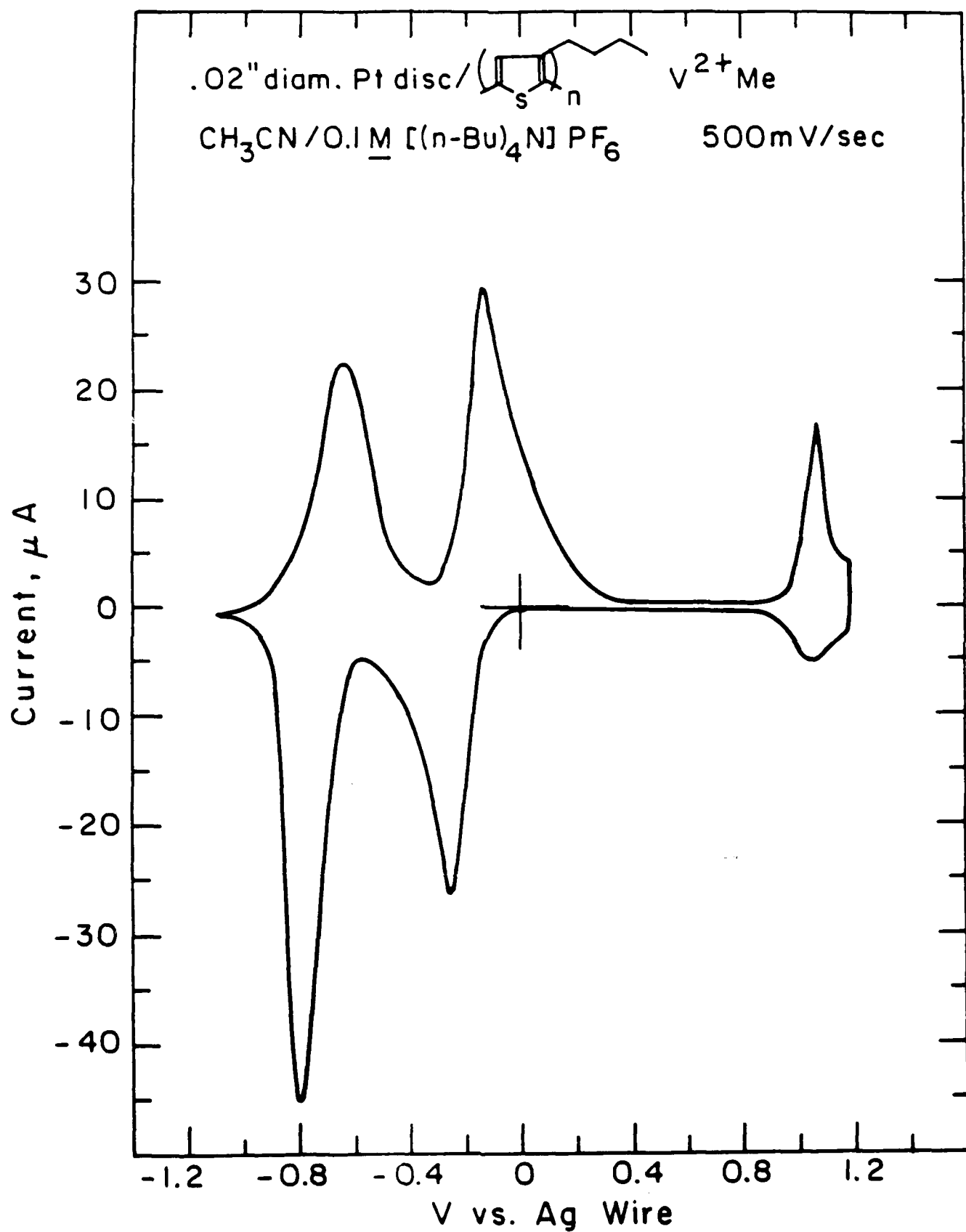
of  $1 \times 10^{-7}$  mole electrons per  $\text{cm}^2$  of area covered by polymer. Bottom:  $I_D-V_G$  characteristic in the same medium for the same pair of derivatized microelectrodes. Maximum conductivity on the positive sweep is  $\sim 10^{-3} \Omega^{-1} \text{cm}^{-1}$ . The window in which conductivity is at least 20% of maximum is at most 2.4 V wide (difficult to determine because of slow redox equilibration by polymer).



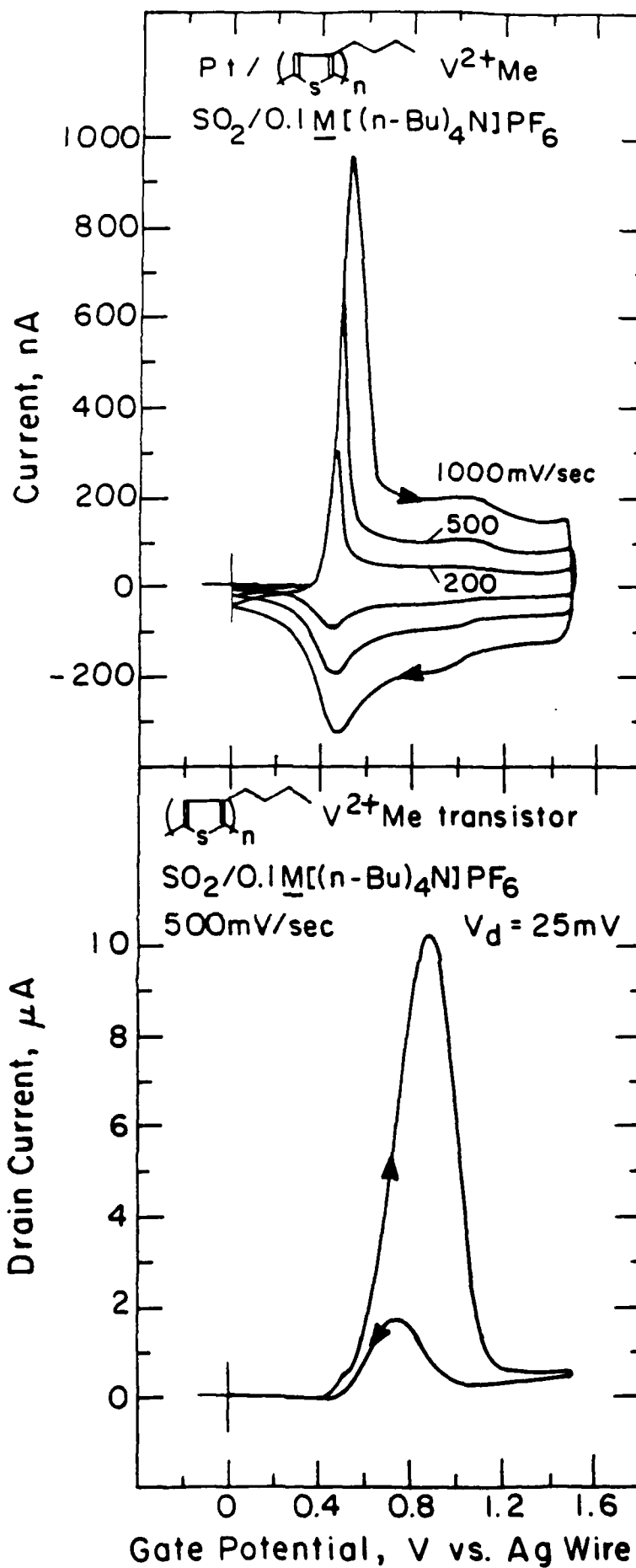


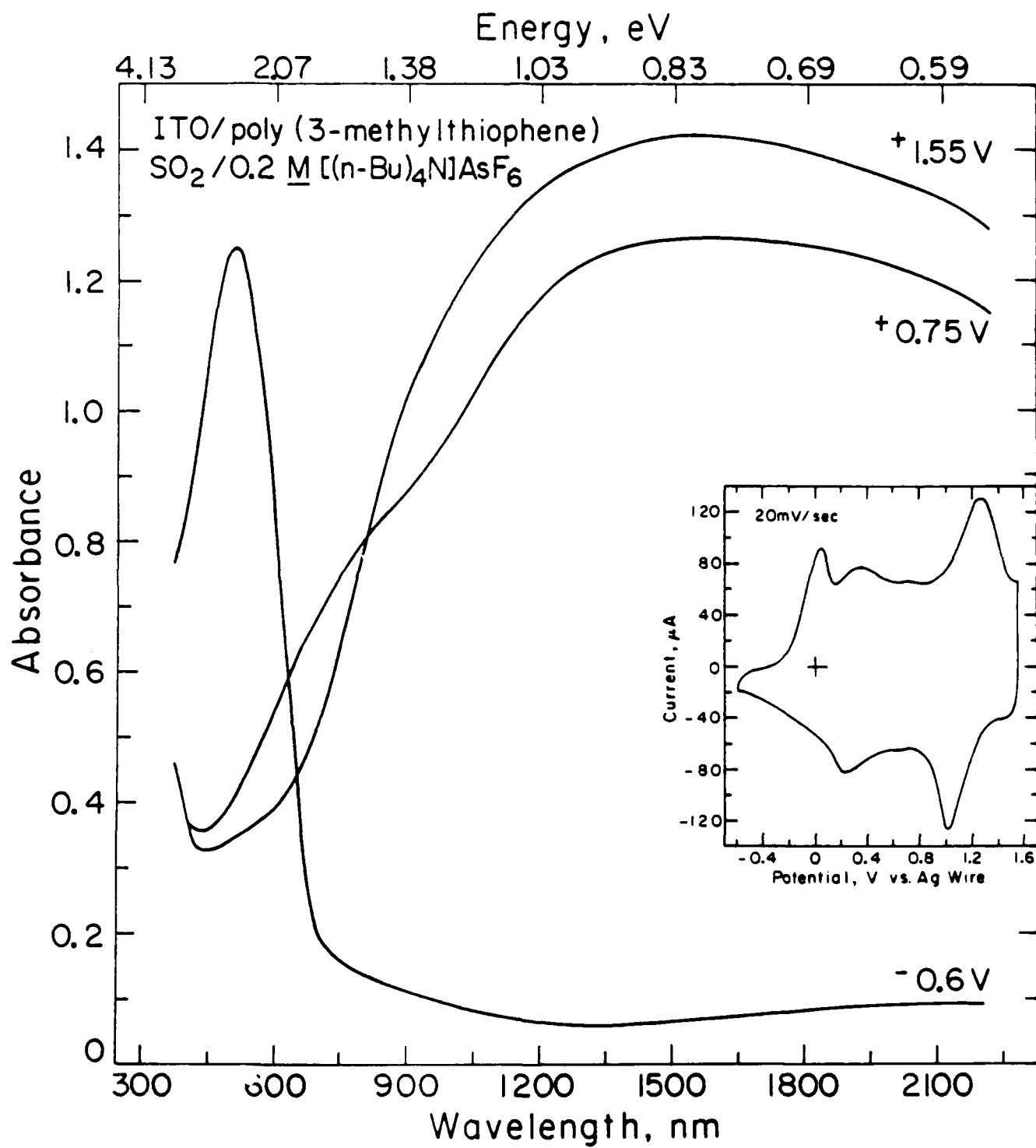


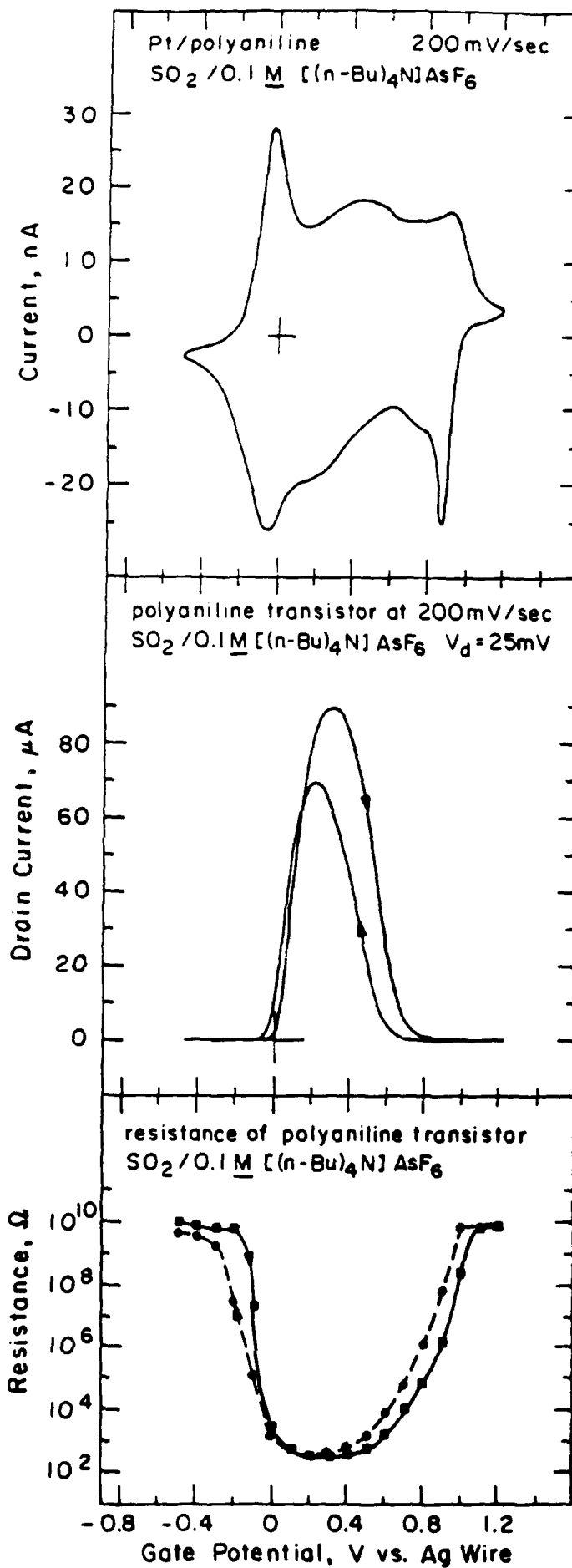


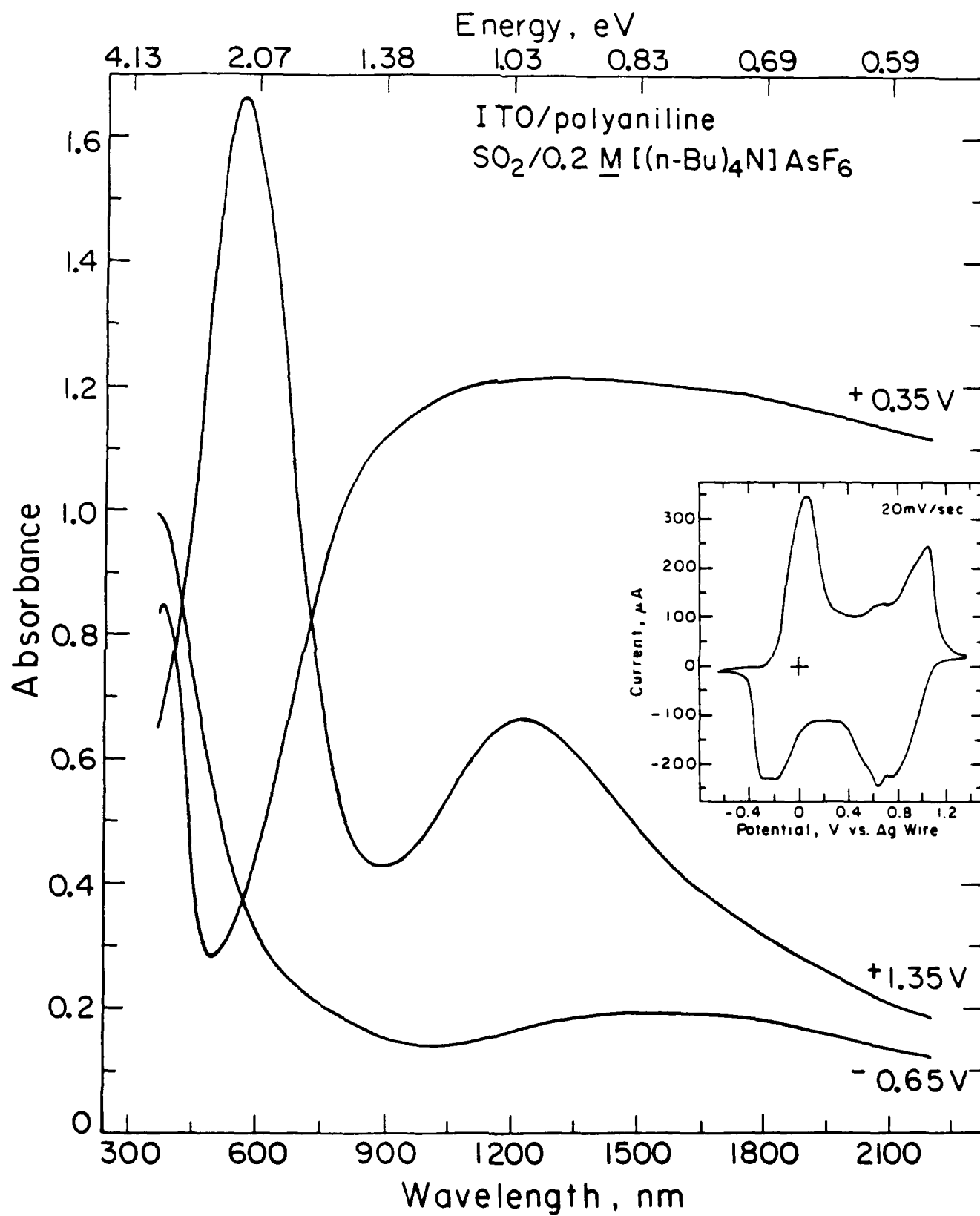


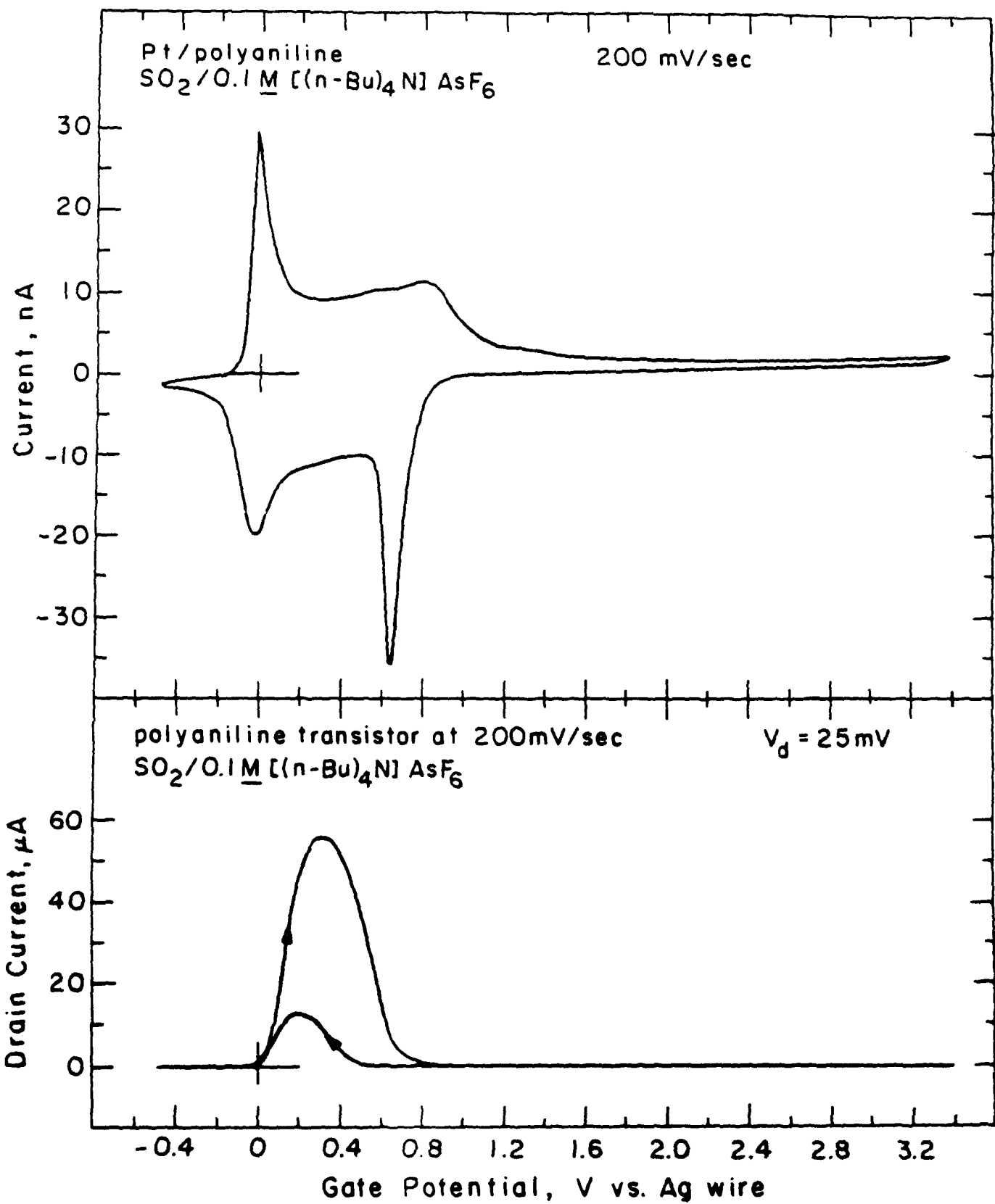


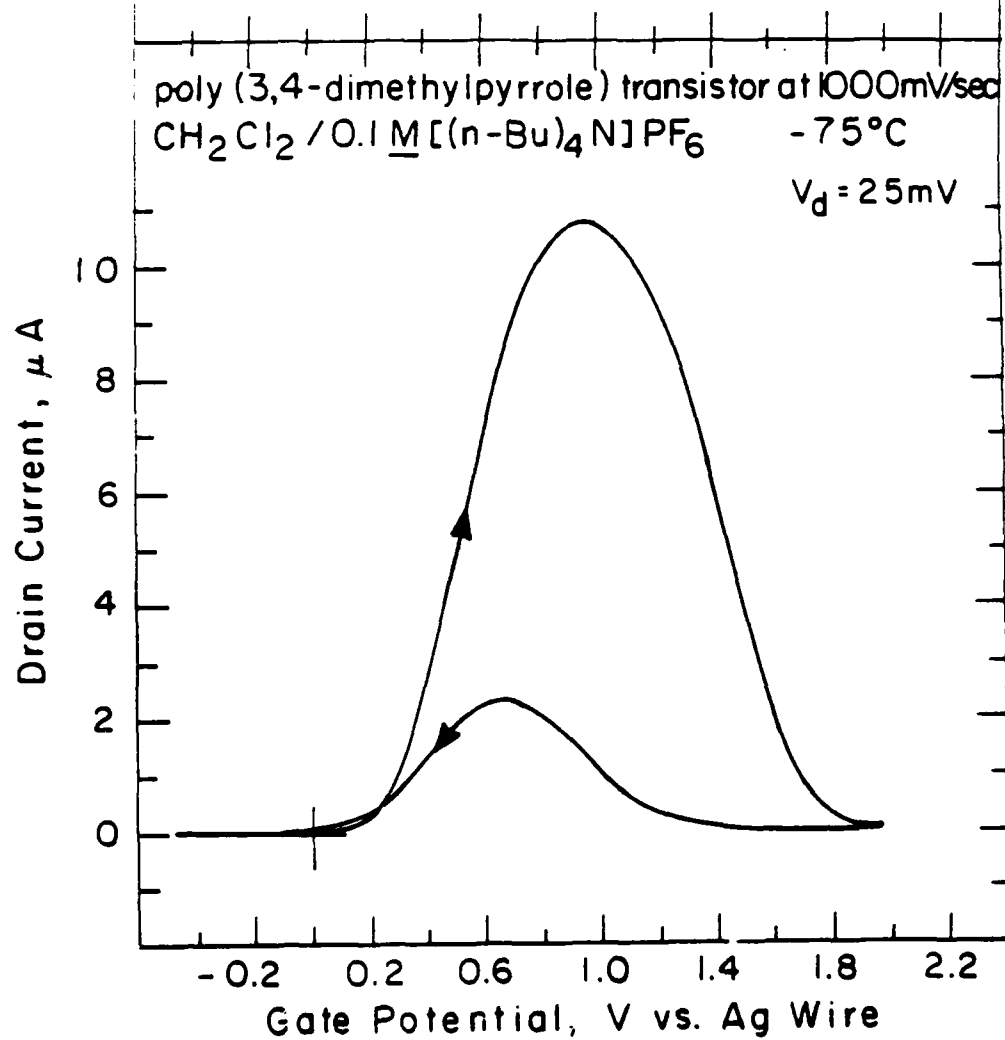
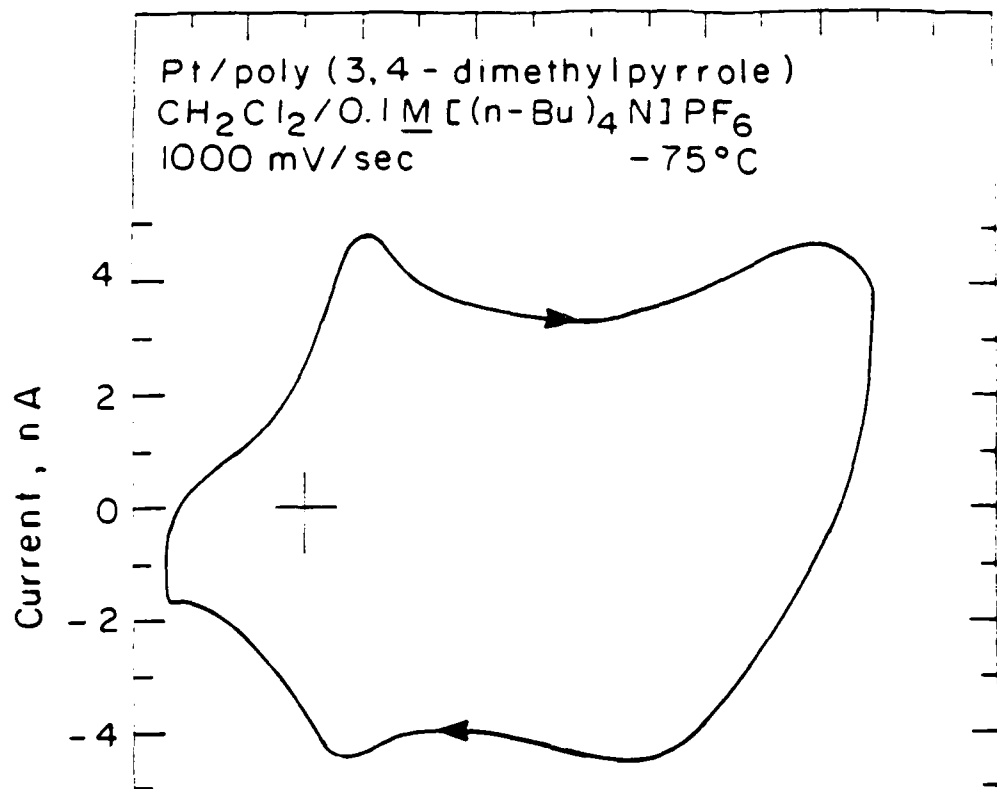


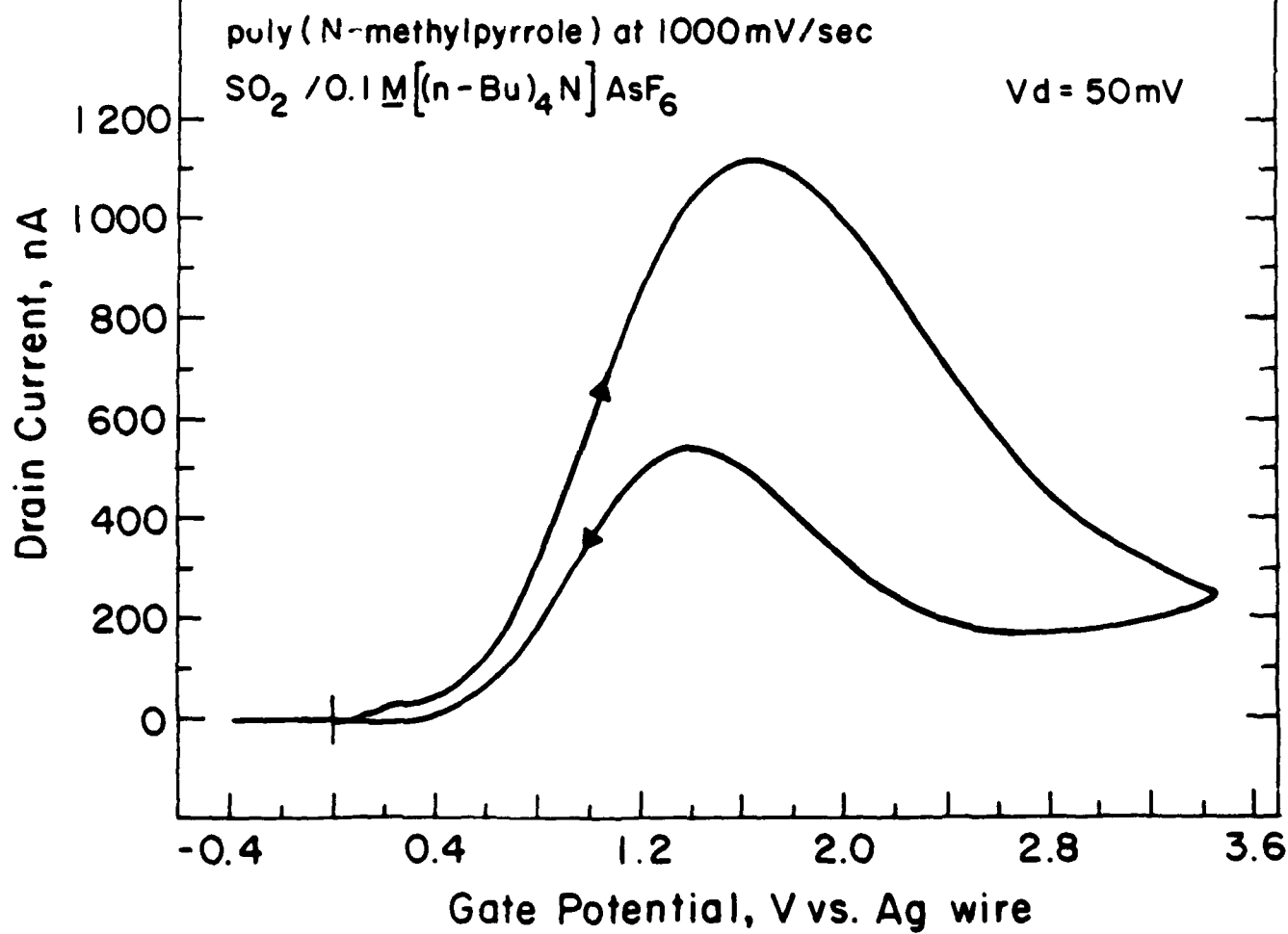
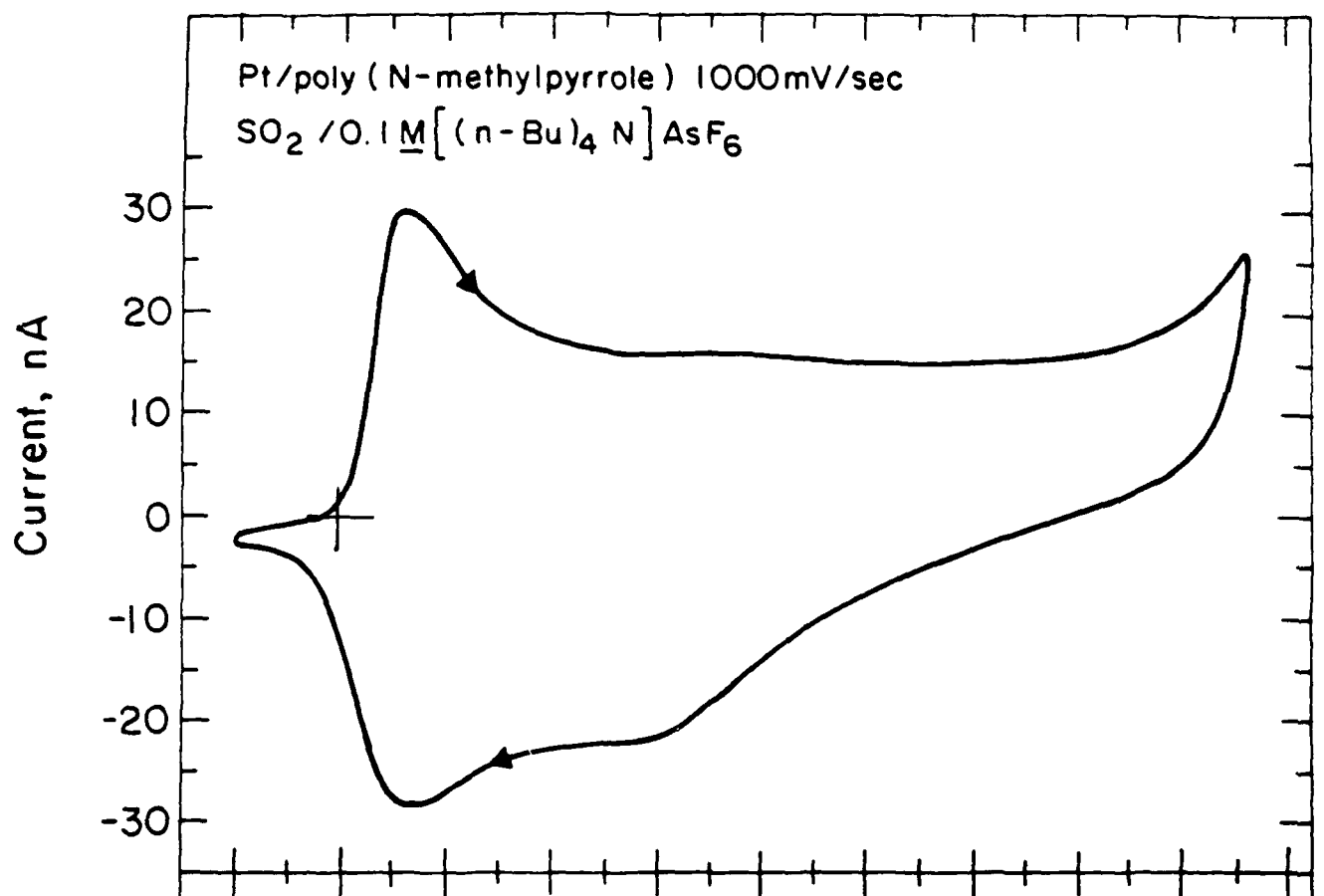












TECHNICAL REPORT DISTRIBUTION LIST - GENERAL

Office of Naval Research (2)  
Chemistry Division, Code 1113  
800 North Quincy Street  
Arlington, Virginia 22217-5000

Commanding Officer (1)  
Naval Weapons Support Center  
Dr. Bernard E. Douda  
Crane, Indiana 47522-5050

Dr. Richard W. Drisko (1)  
Naval Civil Engineering  
Laboratory  
Code L52  
Port Hueneme, CA 93043

David Taylor Research Center (1)  
Dr. Eugene C. Fischer  
Annapolis, MD 21402-5067

Dr. James S. Murday (1)  
Chemistry Division, Code 6100  
Naval Research Laboratory  
Washington, D.C. 20375-5000

Dr. Robert Green, Director (1)  
Chemistry Division, Code 385  
Naval Weapons Center  
China Lake, CA 93555-6001

Chief of Naval Research (1)  
Special Assistant for Marine  
Corps Matters  
Code 00MC  
800 North Quincy Street  
Arlington, VA 22217-5000

Dr. Bernadette Eichinger (1)  
Naval Ship Systems Engineering  
Station  
Code 053  
Philadelphia Naval Base  
Philadelphia, PA 19112

Dr. Sachio Yamamoto (1)  
Naval Ocean Systems Center  
Code 52  
San Diego, CA 92152-5000

Dr. Harold H. Singerman (1)  
David Taylor Research Center  
Code 283  
Annapolis, MD 21402-5067

ENCLOSURE(2)